

CHALMERS



Simulation and Testing of a Switched Reluctance Motor

By Matlab /Simulink and dSPACE

Master of Science Thesis in Electric Power Engineering

Saman Abbasian

Department of Energy and Environment

Faculty of Electric Power Engineering

CHALMERS UNIVERSITY OF TECHNOLOGY

Göteborg, Sweden, 2013

Simulation and Testing of a Switched Reluctance Motor

By Matlab/Simulink and dSPACE

Saman Abbasian

Thesis proposed in fulfillment of the prerequisites

For the Master degree in engineering science

Faculty of Power Electrical Engineering

Chalmers University

August 2013-08-31

Supervisor

Dr. Saeid Haghbin

Examiner

Prof. Torbjörn Thiringer

Department of Energy and Environment

Faculty of Electric Power Engineering

CHALMERS UNIVERSITY OF TECHNOLOGY

Göteborg, Sweden, 2013

Simulation and Testing of a Switched Reluctance Motor

By Matlab/Simulink and dSPACE

SAMAN ABBASIAN

© SAMAN ABBASIAN, 2013

Department of Energy and Environment
Faculty of Electric Power Engineering
CHALMERS UNIVERSITY OF TECHNOLOGY
SE-412 96 Göteborg
Sweden
Telephone: + 46 (0)31-772 1000

Göteborg, 2013

ABSTRACT

Simulation and Testing of a Switched Reluctance Motor

By *Matlab /Simulink* and *dSPACE*

Saman Abbasian

Department of Energy and Environment

Faculty of Electric Power Engineering

Chalmers University of Technology

The main objective of this thesis is to build and test a *SRM* drive system to provide a research platform for having more investigations in this field. First, a literature study of switched reluctance motors which includes fundamental operation, control techniques and energizing methods is done and second, a linear magnetic mathematical model is developed in *Matlab / Simulink* to analysis the dynamic response of the machine using a *PI* speed controller and a feedback control system under different working conditions.

A voltage source strategy is applied to the *SRM* and since each phase is controlled by pulses of current during the torque production with a repeating sequence, it is important to calculate the turning on, θ_{on} , and off, θ_{off} , angles properly. In addition, a hysteresis current controller is required to maintain the current within a preset band.

To operate the *SRM*, an experimental setup and an assembly of *PCB* are needed. These boards are the main part of the project and they are controlled by a *dSPACE* system. Simultaneously, protection and measurement units are used to monitor *SRM* drive in faulty situations.

Finally, an open loop control is implemented in a real time environment and practical results are compared with theories to obtain a good assessment of the system.

Acknowledgments

No one is perfect and no work is made by a single man.

I would like to dedicate my special thanks to my great supervisor, Dr. Saeid Haghbin for his endless patience and support which helped me to finish my Master thesis. I never forget his teaching method that was an inspiration of new experiences.

I must also express my gratitude to Prof. Torbjörn Thiringer who gave me this great opportunity to do my Master project in the Electric Power Engineering Department of Chalmers University of Technology and his useful comments in writing my report. Thanks to the division of electric power engineering which paved the way for me by providing required equipment and enough facilities. Other special thanks go to Yi Du for his support in practical set up.

In my daily activities I was assisted by the other friendly and cheerful group of Post Doc and PhD staffs: Tarik Abdulahovic, Ali Rabiei as well as many other friends in this department.

Last but not least, infinite appreciation goes to my mother for her endless prayers.

Saman Abbasian

Göteborg, Sweden

Wednesday, August30, 2013

List of symbols, abbreviations

Abbreviations

<i>SRM</i>	Switched Reluctance Motor
<i>VSC</i>	Voltage Source Control
<i>CSC</i>	Current Source Control
<i>CCT</i>	Current Control Technique
<i>SCT</i>	Speed Control Technique
<i>PCB</i>	Printed Circuit Board
<i>HCC</i>	Hysteresis Current Control

Symbols

B	Friction Coefficient
ΔW_{elec}	Incremental Energy Delivered
$\Delta W_{storage}$	Incremental Energy Stored
ΔW_{mech}	Mechanical Work
T_{em}	Electromagnetic Torque
N_r	Number of Rotor Poles
N_s	Number of Stator Poles
β_s	Stator Pole Angle
β_r	Rotor Pole Angle
L_u	Minimum Inductance in Unaligned Position
L_a	Maximum Inductance in Aligned Position

D_{so}	Stator Outer Diameter
D_{si}	Stator Inner Diameter
N_r	Number of Rotor Poles
D_{ro}	Outer Rotor Diameter
D_{ri}	Inner Rotor Diameter
Y_{sth}	Stator Yoke Thickness
Y_{rth}	Rotor Yoke Thickness
l_{airgap}	Air Gap Length
θ_{on}	Turning On Angle
θ_{off}	Turning Off Angle
T_L	Load Torque
T_e^*	Torque Command
ω_{ref}	Reference Speed
ω_{error}	Speed Error
I_{dc}	DC Link Current
$L(\theta)$	Phase Inductance
J	Moment of Inertia
I_m	Saturation Current
V_{dc}	DC Link Voltage
φ	Flux Linkage

List of figures

Figure 2.1: Cross section of a three phase switched reluctance motor (SRM), unaligned rotor position.....	3
Figure 2.2: Cross section of a three phase switched reluctance motor (SRM), unaligned rotor position.....	4
Figure 2.3: $B - H$ curve for different rotor positions, aligned and unaligned positions.....	4
Figure 2.4: Co-energy graph between aligned and unaligned rotor situations.....	5
Figure 2.5: An ideal phase inductance versus rotor position.....	6
Figure 2.6: Inductance profiles for three phases.....	7
Figure 2.7: Equivalent circuit for phase a.....	11
Figure 2.8: power converter unit.....	11
Figure 2.9: Estimation of the rotor position by the flux linkage calculation.....	12
Figure 2.10: Flux linkage versus current curves... ..	12
Figure 2.11: Voltage control technique.....	13
Figure 2.12: Voltage and current profiles.....	13
Figure 2.13: Current control technique.....	14
Figure 2.14: Voltage and current profiles.....	14
Figure 2.15: Hysteresis current controller.....	15
Figure 3.1: Test set-up to measure the stator resistance of a SRM.....	16
Figure 3.2: Test set-up to measure the aligned and unaligned inductances of a SRM.....	17
Figure 3.3: Maximum and minimum inductances simulated by the software.....	20
Figure 3.4: Geometry of the SRM.....	20
Figure 4.1: Mechanical drive of the motor system.....	21
Figure 4.2: The main diagram of the speed control of a SRM.....	22
Figure 4.3: PI controller with an anti-wind up.....	23

Figure 4.4: Simulink block of the Speed control of the SRM.....	25
Figure 4.5: Controlling of Phase A.....	25
Figure 4.6: Motor speed and speed command without the load effect.....	28
Figure 4.7: Motor speed and speed command with the load effect.....	28
Figure 4.8: Magnified motor speed and speed command without the load effect.....	29
Figure 4.9: Magnified motor speed and speed command with the load effect.....	29
Figure 4.10: Motor speed and speed command with the effect the load during a time interval.....	30
Figure 4.11: Changing the load torque during a time interval from 4 to 1N.m	30
Figure 4.12: Motor speed and speed command with the load effect during a time interval.....	31
Figure 4.13: Changing the load torque during a time interval from 1 to 4N.m.....	31
Figure 4.14: Motor speed and speed command without the load effect four quadrants.....	32
Figure 4.15: Motor speed and speed command with the load effect four quadrants.....	32
Figure 4.16: Magnified motor speed and speed command without the load effect four quadrants.....	33
Figure 4.17: Magnified motor speed and speed command with the load effect four quadrants.....	33
Figure 4.18: Motor speed and speed command without the load effect four quadrants.....	34
Figure 4.19: Motor speed and speed command with the load effect four quadrants.....	34
Figure 4.20: Magnified motor speed and speed command without the load effect four quadrants.....	35
Figure 4.21: Magnified motor speed and speed command with the load effect four quadrants.....	35
Figure 4.22: Current in phase A with the load effect at speed of 1000 rpm.....	36
Figure 4.23: Torque in phase A with the load effect at speed of 1000 rpm.....	36
Figure 4.24: Current in phase B with the load effect at speed of 1000 rpm.....	37
Figure 4.25: Torque in phase B with the load effect at speed of 1000 rpm	37

Figure 4.26: Current in phase C with the load effect at speed of 1000 rpm	38
Figure 4.27: Torque in phase C with the load effect at speed of 1000 rpm....	38
Figure 4.28: Three phase currents A,B,C with the load effect at speed of 1000 rpm	39
Figure 4.29: Total electromagnetic torque A,B,C with the load effect at speed of 1000 rpm... ..	39
Figure 5.1: General schematic of the whole system.....	40
Figure 5.2: Switched Reluctance Motor <i>SRM</i>	42
Figure 5.3: Single <i>PCB</i>	42
Figure 5.4: Three power converter boards.....	43
Figure 5.5: Embedded <i>PCB</i> for operation.....	44
Figure.5.6: Voltage and current transducers in the measurement box unit.....	44
Figure 5.7: Current in phase A	45
Figure.5.8: Three phase currents A, B, C.....	46

Table of contents

Title.....	i
Abstract.....	iv
Acknowledgments.....	v
List of symbols,abbreviations.....	vi
List of figures.....	viii
CHAPTER 1 INTRODUCTION.....	1
1.1 Background Study.....	1
1.2 Objective of the Research.....	2
1.3 Outline and Objectives of the Research.....	2
CHAPTER 2 THREE PHSES SWITCHCED RELUCTANCE MOTOR.....	3
2.1 Construction and Principle of Operation of SRM.....	3
2.2 Torque Production in a SRM.....	5
2.3 Relationship Between Inductance and Rotor Position.....	6
2.4 Designing Criteria Parameters.....	8
2.5 Selection of Rotor and Stator Pole Arcs.....	9
2.6 Dynamic Model of a SRM.....	10
2.7 Control Strategy.....	11
2.8 Energizing Strategies.....	13
CHAPTER 3 PARAMETER ESTIMATION OF SRM.....	16
3.1 Determination of the Inductance and Resistance Values of SRM.....	16
3.2 Comparison of the Practical Measurements With Maxwell Software.....	17

CHAPTER 4 SPEED CONTROL OF THE SWITCHED RELUCTANCE MOTOR.....	21
4.1 Mechanical Model with Friction.....	21
4.2. Matlab/ Simulink Simulation of Speed Control.....	21
4.3. PI speed Controller with an Anti wind up.....	23
4.4. Simulation Results	26
CHAPTER 5 EXPERIMENTAL SETUP	40
5.1 SRM Setup Installation.....	40
5.2 Hardware Used in the Lab.....	41
5.3 Switched Reluctance Motor.....	41
5.4. Printed Circuit Boards <i>PCB</i>	42
5.5 Measurement Units of Voltages and Currents.....	44
5.6 Practical Results For an Open Loop Performance.....	45
Chapter 6 CONCLUSION AND FUTURE WORK.....	47
6.1 Conclusions.....	47
6.1 Future Work.....	47

Chapter 1

INTRODUCTION

1.1 Background Study

One of the most important criteria for designing an electric drive system is to have a good knowledge of the motor dynamic behavior. Additionally, the method in which an electrical motor interacts with power electronic converters must be studied. Therefore, power converters are used to achieve the desired torque and speed from the motor. In comparison with other drive systems such as combustion engines and hydraulic engines, electric drives have a very wide field of applications and also advantages of making a large speed control range, little acoustic noise operation and versatile control ability.

Among the electrical machine drives such as induction motor drives, DC motor and permanent magnet synchronous motor drives, SRM drives are growing rapidly in numbers. Perhaps one of the simplest electrical machines due to its construction, where only stator windings and a magnetic rotor in a saliency form are used. In the late 70, popularity of concepts of these type machines was fostered with the assistance of fast development switching technologies [8].

Even though the construction is simple, the control is not an easy task for the SRM since the phase energizing should be implemented at the right angle, in order to have less speed oscillations. Another issue is the double saliency construction on the both rotor and stator, so that torque production by separate phase's results in large torque ripples [3]. This effect also produces a current ripple in the DC supply and to a demand of a large filter capacitor. In addition, another negative effect of the torque ripple is the acoustic noise, due to the induced radial magnetic forces.

Fortunately, the power electronics and microprocessors recently have done good advancements and more accurate control in this field that allows these kinds of machines to be controlled precisely and become competitive with the other motor technologies in the vast range of industrial applications.

To sum up, SRMs are cheap, robust, no winding in the rotor, have a very simple construction and fault tolerant. However, for an operation speed and torque, the stator current must be turned on and off at a right rotor position to produce the desired torque which requires a precise control algorithm.

1.2 Objective of the Present Work

It is intended to build up and simulate a SRM drive system based on *Matlab / Simulink* with the assistance of *dSPACE* to develop a model that can be used later for a closed loop speed control system.

The procedure is summarized as follows;

- 1- Simulation of a *SRM* drive system in *Matlab*
- 2- Parameter's measurement of a *SRM*
- 3- Assembly of the hardware: printed circuit boards, current and voltage measurement units
- 4- Testing the experimental setup
- 5- Performing an open loop control method by using *Matlab* and *dSPACE*

1.3 Outline of the Research Approach

A summary of this thesis is as follows

An overview of a three phase SRM which can be found in Chapter 1. It is followed by Chapter 2, in which elementary operation, principals, mathematical equations for torque production, derivation of the inductance and rotor positions are discussed. In Chapter3, a brief overview about the designing parameters criteria of the machine such as pole selection, stator and rotor pole angle selection are presented. Determination of the inductance and resistance values of the machine is also explained.

In Chapter 4 a method of the control is discussed in detail. A *Matlab* simulation project which would be the core part presents how to control the actual speed to the reference speed and using the relevant equations to model the dynamic response of a three phase *SRM* . Practical analysis, experimental setup hardware such as *PCB* , current sensors, protection units and *dSPACE* are explained in Chapter 5. In addition, observations are demonstrated and conclusions are based according to these results. Finally, Chapter 6 deduces the entire activities performed in this thesis by a summary of the activities and discussions about future research work.

Chapter 2

THREE PHSES SWITCHCED RELUCTANCE MOTOR

2.1 Construction and Principal of Operation of (SRM)

A cross section of a three phase switched reluctance motor (SRM) is shown in Fig. 2.1 and 2.2 respectively. In order to achieve a continuous rotation, each phase winding is energized by a proper current at a suitable rotor angle. It means that the excitation is done sequentially from phase to phase as the rotor moves.

Assume that the rotor poles R_2, R'_2 and stator poles are in an aligned position. When the phase winding A is energized by applying a current, flux passes within the stator poles A and A' and rotor poles R_2 and R'_2 and it causes a force that pulls the rotor poles towards the stator poles A and A' . After alignment, rotor poles R_2 and R'_2 with the stator poles the stator current of the phase A is turned off and Fig. 2.2 show this variation.

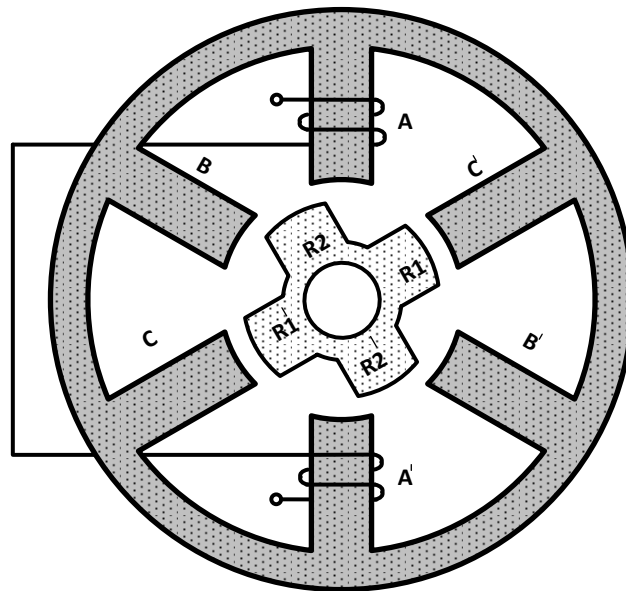


Figure 2.1: Cross section of a three phase SRM, unaligned rotor position

This is the reason why the machine is called SRM. When the rotor is aligned with the stator poles, the air-gap distance is small and inductance is large. The method of movement of the rotor is implemented by switching of the converter and it explains the name, the SRM.

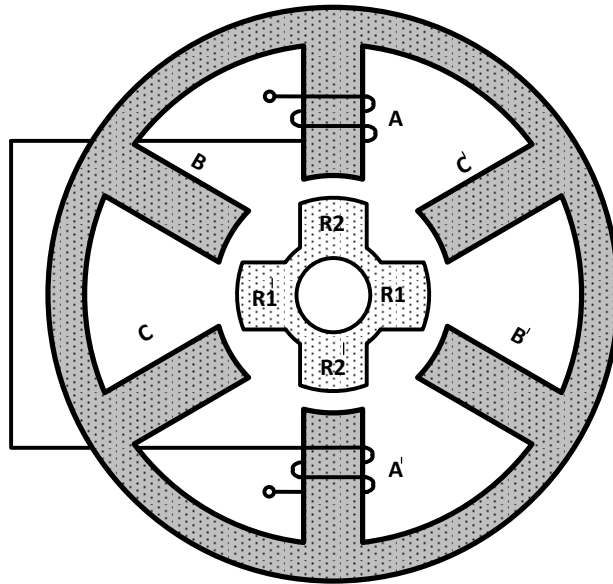


Figure 2.2: Cross section of a three phase SRM, aligned rotor position

The $B - H$ curve for the unaligned and aligned position is shown in Fig. 2.3.

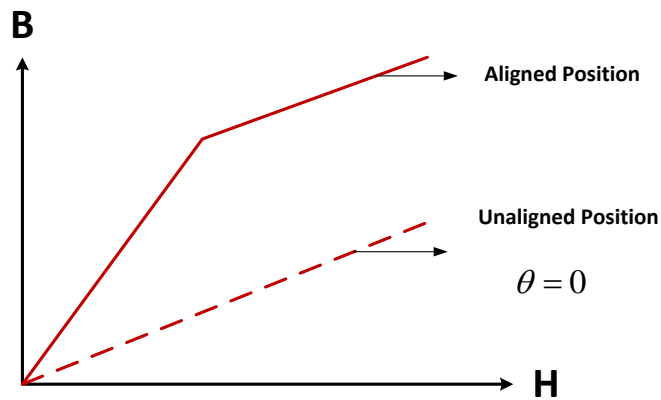


Figure 2.3: $B - H$ curve the aligned and unaligned positions

2.2 Torque Production in a SRM

Applying a current i_A as shown in Fig. 2.4 keeping the rotor at a position θ_1 between the unaligned and aligned positions, the instantaneous electromagnetic torque is determined as follows

Allowing the rotor to move incrementally under the influence of the electromagnetic torque from position θ_1 to $\theta_1 + \Delta\theta_{mech}$, holding the current constant i_A results in the equation:

$$\Delta W_{mech} = T_{em} \Delta\theta_{mech}. \quad (2.2.1)$$

The incremental energy delivered by the electrical source is the equation:

$$\Delta W_{elec} = \text{area}(1-2-\lambda_2-1). \quad (2.2.2)$$

Where λ_1 and λ_2 are flux linkages at two rotor positions.

The area above is the incremental energy stored with corresponding winding so

$$\Delta W_{storage} = \text{area}(0-2-\lambda_2-0) - \text{area}(0-1-\lambda_1-0). \quad (2.2.3)$$

The mechanical work done is the difference between the electrical energy and energy stored

$$\Delta W_{mech} = \Delta W_{elec} - \Delta W_{storage}. \quad (2.2.4)$$

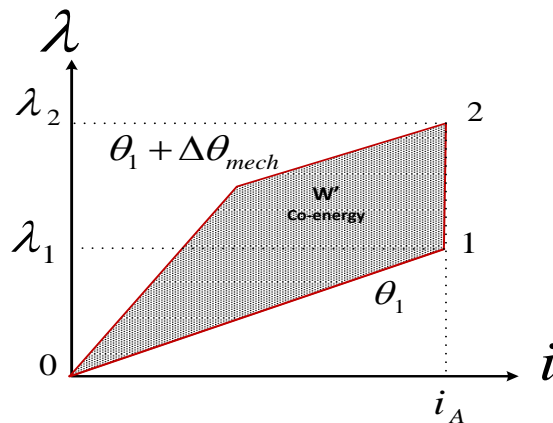


Figure 2.4: Co-energy graph between aligned and unaligned rotor situations

Therefore, the mechanical work done is equal to the co-energy between two rotor positions 1 and 2. Hence, the electromagnetic torque as a function of the rotor position and the current is

$$T_e = \frac{\partial W'}{\partial \theta}. \quad (2.2.5)$$

Since the torque is a nonlinear function of the phase current and rotor position as shown in Fig. 2.4, (2.2.5) is rewritten in the form of inductance variation from the unaligned to the aligned position

$$T_e = \frac{1}{2} i^2 \frac{dL}{d\theta}. \quad (2.2.6)$$

Clearly, it can be seen that the average torque is developed through the tendency of the magnetic circuit to adopt a configuration of minimum reluctance for the rotor poles.

Some important hints can be seen from (2.2.6):

- 1- Torque is proportional to the square of the current. Regardless of the current direction torque can be produced in both directions.
- 2- Electromagnetic torque is very similar to a series DC machine that has a prominent starting torque.
- 3- Due to the independence of each phase from an electrical standpoint, during a faulty condition such as a short circuit in one phase, there won't be any effect on the other phases.
- 4- The role of the saturation is vital, because of in each excitation cycle a large ratio of the energy supplied to a phase winding that is required to be converted into the mechanical work.

2.3 Relationship between the Inductance and Rotor Position for a 6/4 SRM

An ideal phase inductance versus rotor position is illustrated in Fig. 2.5.

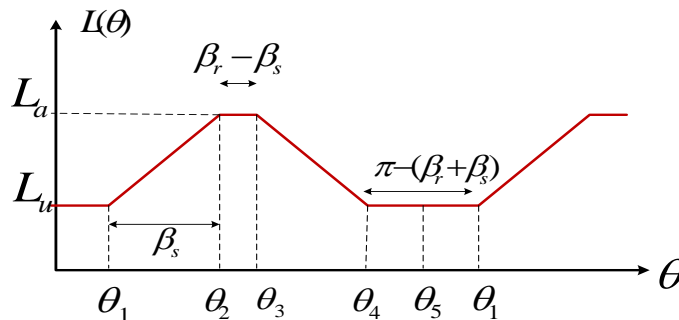


Figure 2.5: An ideal phase inductance versus rotor position

where

$$\theta_1 = \frac{1}{2} \left[\frac{2\pi}{N_r} - (\beta_s + \beta_r) \right]. \quad (2.3.1)$$

$$\theta_2 = \theta_1 + \beta_s. \quad (2.3.2)$$

$$\theta_3 = \theta_2 + (\beta_r - \beta_s). \quad (2.3.3)$$

$$\theta_4 = \theta_3 + \beta_s. \quad (2.3.4)$$

$$\theta_5 = \theta_4 + \theta_1 = \frac{2\pi}{N_r}. \quad (2.3.5)$$

Fig. 2.7 illustrates three phase inductance profile for the 6/4 SRM used in this project.

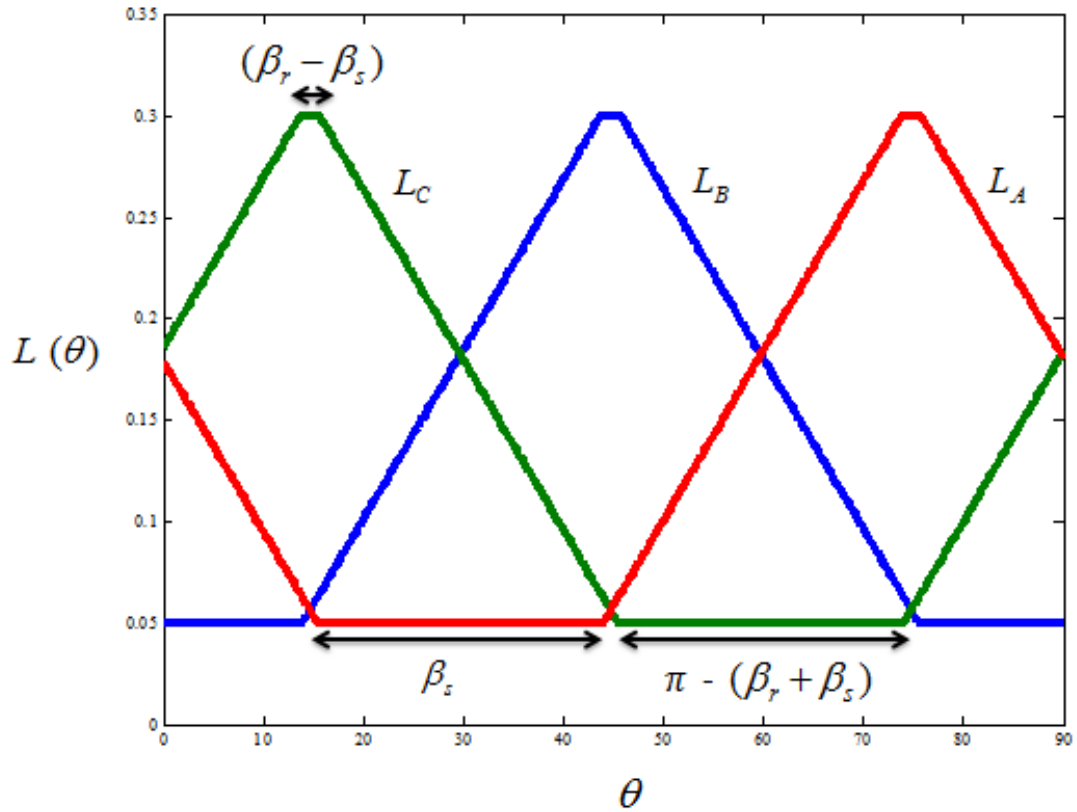


Figure 2.6: Inductance profiles for three phases of the SRM

Table 2.3.1: Torque production as a function of the inductance variations

Rotor angles	Results
$0 - \theta_1$ and $\theta_4 - \theta_5$	No overlap between the stator and rotor, minimum inductance, no torque production
$\theta_1 - \theta_2$	Poles overlap, inductance increases with positive slope, a positive torque production
$\theta_2 - \theta_3$	Not alter an overlap between the stator and rotor, keeping the inductance maximum constant, torque generation zero
$\theta_3 - \theta_4$	Rotor pole moving away from overlapping, decreasing the inductance, negative slope, negative torque production

The above idealized presentation has shown the fundamental principle of a SRM. But in real motors, the actual inductance profile will have a rounding in the transition areas due to the magnetic saturation when the flux density increases in the ferromagnetic material as pole alignment occurs. Moreover, the coil currents will have the same delay rounding in the leading edges which resulting in ripples in the total electromagnetic torque development.

2.4 Designing Criteria Parameters

One of the major issues in the pole selection is the number of power converter switches. In fact, it is a limiting factor in terms of cost of the power processing unit which will affect on the control of a small rise and fall times of the phase current. Another important aspect is the relation between the stator frequency and the number of rotor poles according to the expression below [1],

$$f_s = \left(\frac{\omega_{rm}}{2\pi}\right)P_r (Hz). \quad (2.4.1)$$

Table 2.4.1: Number of stator and rotor poles of SRM

	Poles			
Stator	6	8	12	12
Rotor	4	6	8	10

By increasing the rotor poles the stator frequency increases which will result a higher core losses and a prolonged conduction time for the rising and falling of the phase current. In addition, it needs more windings in the stator periphery that increase the cost of designing for the power control processor unit.

2.5 Selection of the rotor and stator pole arcs

Since, it takes more time to show the procedure for obtaining the final expression for rotor and stator pole arcs selection, here only the fundamental equation is shown according to the expression below [1],

$$(\beta_r - \beta_s) \geq 0. \quad (2.4.2)$$

where the minimum stator pole angle is according to [1],

$$\min[\beta_s] = \frac{4\pi}{N_s N_r}. \quad (2.4.3)$$

Therefore, (2.4.2) specifies that the rotor pole arc has to be greater than or at least equal to the stator pole arc and simplified in the form of:

$$\beta_r \geq \beta_s. \quad (2.4.4)$$

To summarize, the importance of the angle selection is a necessity in the design procedure of a SRM. Since the machine operation is based on the inductance variation in the different rotor positions, it requires another equation which provides a necessary constraint of having an inductance normal profile. The equation is shown according to [1],

$$\left(\frac{2\pi}{N_r} - \beta_r\right) \geq \beta_s. \quad (2.4.5)$$

If this condition is not held, the inductance profile of the machine will not be normal.

2.6 Dynamic Model of a Switched Reluctance Motor

Due to the non-linearity in a SRM, usually a simplified model of the motor is used.

Therefore, a simplified equivalent circuit for a switched reluctance motor might be derived by ignoring the mutual inductance between the phases. In order to make a dynamic model for this motor, the equation is the applied voltage to a phase which is the sum of the resistive voltage drop, the derivative of the flux linkages as a function of the rotor position and the current.

$$V = R_s i + \frac{d\lambda(\theta, i)}{dt}. \quad (2.6.1)$$

Assume that the poles of those phases are in an unaligned position where the inductance value is small. Equation (2.6.1) expresses an equivalent $R-L$ circuit but due to the nature of nonlinearity of inductance, when the poles move from an unaligned position to an aligned position, a simple mathematical expression cannot verify the current trajectory.

So, (2.6.1) for phase A can be rewritten in the same way as

$$V = R_s i_A + \frac{d\lambda_A(\theta, i_A)}{dt} \frac{di}{dt} + \frac{d\lambda_A(\theta, i_A)}{d\theta} \omega_m. \quad (2.6.2)$$

The above equation can be modified as follows to

$$kV_t = R_s i_A + L_A(\theta, i_A) \frac{di}{dt} + K(\theta, i_A) \omega_m. \quad (2.6.3)$$

Where k indicate the state of the power converter switches for the values of

$$k = \pm 1. \quad (2.6.4)$$

The switches are on when $k = +1$ and off when $k = -1$ and the coefficient of the speed term K can be expressed as a back EMF that depends on the value of the changes in the coil flux linkage with position at the instantant of θ, i_A .

Based on the above equations, an equivalent circuit for phase A is shown in Fig 2.9.

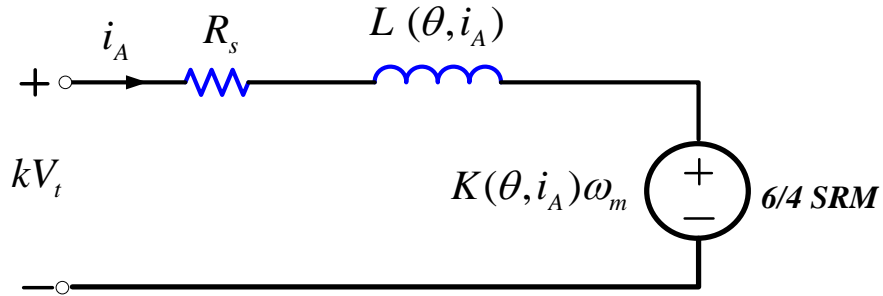


Figure 2.7: Equivalent circuit for phase A

This above model is used in the simulations to investigate the behavior of the motor under different kinds of situation such as loaded and unloaded operation.

2.7 Control Strategy

Despite of the other electrical machines drives which use symmetrical power converters, an asymmetric power converter should be used to control the SRM. There are different types of topologies that have been proposed in the literature [1]. Depending on the machine's phases, a power processing unit can be designed to control each phase independently. Fig. 2.10 represents one of the mostly used converter topologies.

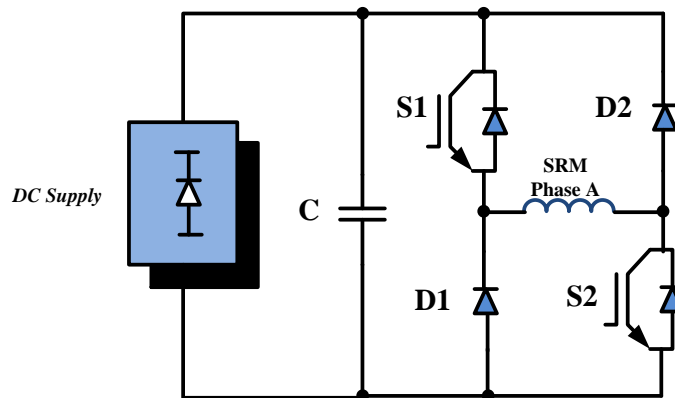


Figure 2.8: Power converter unit for a SRM: asymmetric H-bridge converter

The procedure is to build up a current by turning on both transistors simultaneously, so that the poles of the rotor can be forced towards an aligned position. In order to maintain the current value within a hysteresis band almost near to its reference value, when the poles are aligned, both transistors should be switched off. Then the current flows into the dc bus through the diodes and there is a large energy stored

in the magnetic field of the coil and must be sent back to the dc source consequently, the current decreases in magnitude.

As was mentioned earlier, the rotor position in a switched reluctance motor plays a necessary role to operate it. The turning on, θ_{on} , and turning off, θ_{off} , angles must be chosen to build up a current and then let it decays to operate the motor. One of the easiest controlling methods is presented in Fig. 2.11.

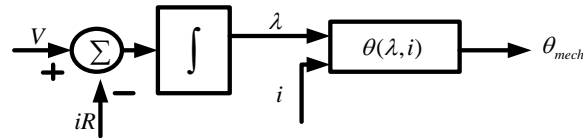


Figure 2.9: Estimation of the rotor position by the flux linkage calculation

Fig. 2.11 above shows how the rotor position can be estimated by computation of the flux linkage of an energized phase by integrating the difference between the applied phase voltage and voltage drop on the resistance of the winding. It means that the flux linkage as a function of the phase current determines the rotor position. Fig. 2.12 shows the family curves of flux linkages as a function of the phase current for different rotor positions.

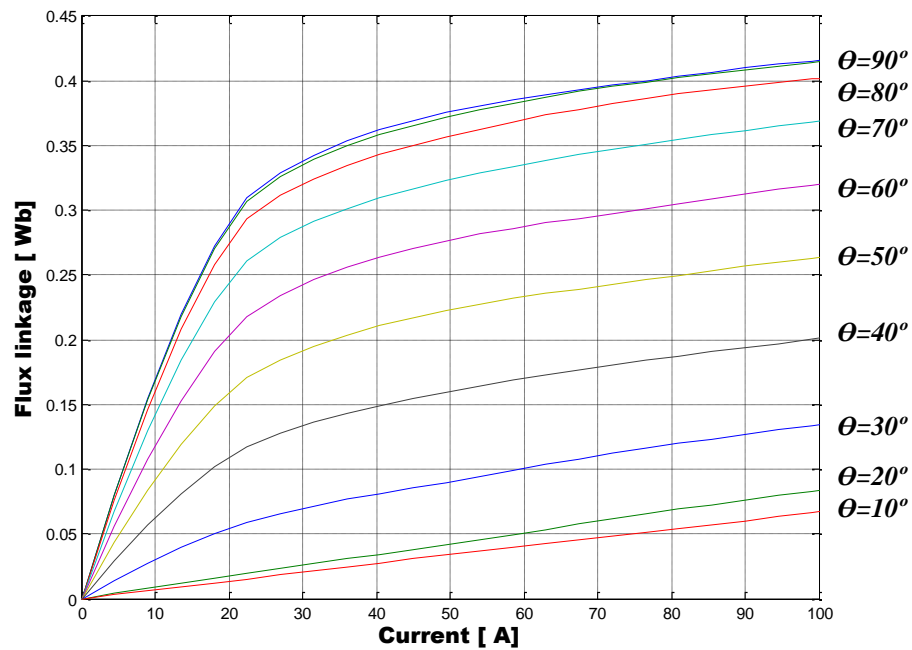


Figure 2.10: Flux linkage versus current curves

2.8 Energizing Strategies

Two most common strategies are as follows

- 1- Voltage source control
- 2- Current controller

In the first method, the *voltage source technique*, the control is implemented by applying the voltage source to a phase winding at turning on angle θ_{on} until a turning off angle θ_{off} . Then, the applied voltage is controlled directly by a speed controller which estimates the speed error after comparison of the desired speed with actual speed and then generates the required phase voltage. Fig. 2.13 illustrates the voltage control technique. The current and the voltage profiles respectively are shown in Fig. 2.14.

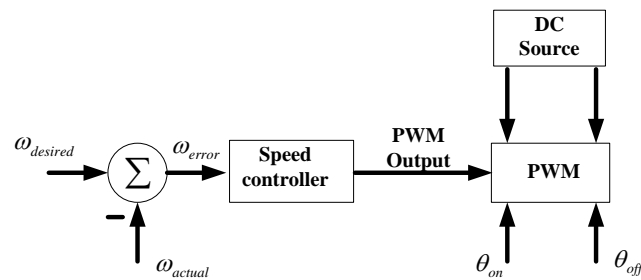


Figure 2.11: Voltage control technique

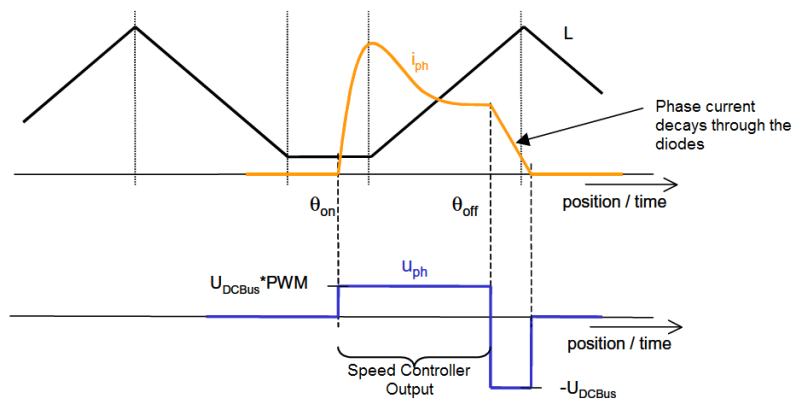


Figure 2.12: Voltage and current profiles

Since the energy stored in the winding needs to be fed back to the source, the applied voltage should be reversed until a certain demagnetizing angle θ_d .

In the second method, the *Current controller technique*, the applied voltage utilized to the machine phases is modulated to achieve the desired current at the energized phase. Then, this applied voltage is monitored by a current controller with an external speed control loop. The speed controller evaluates the speed error after comparison of the desired speed with actual speed and then generates the reference for the phase current. Then, the current controller estimates the difference between the desired and actual phase current and determines the proper *PWM* duty cycle.

Fig. 2.15 and 2.16 illustrate the current control technique and voltage current profiles.

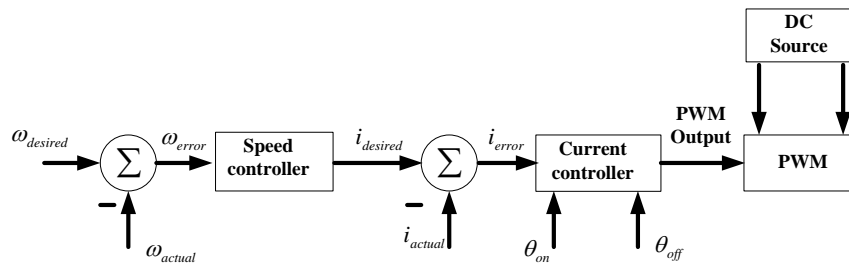


Figure 2.13: current control technique

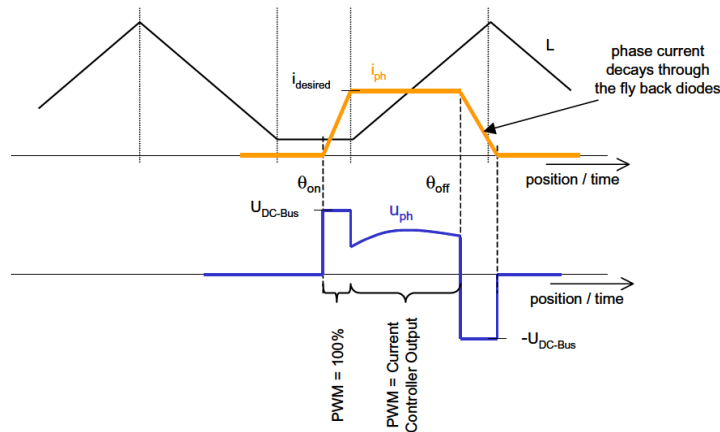


Figure 2.14: Voltage and current profiles

Note that in this method the actual current is permitted to change around the desired reference current according to the permissible current ripple in the tolerance band. In fact, the actual current should be

forced to stay within a tolerance band. Hence, the actual current surpasses either the upper or lower boundary of the tolerance band; the controller modifies the state so that the current returns to the reference value. Fig.2.17. shows a hysteresis current controller for one phase.

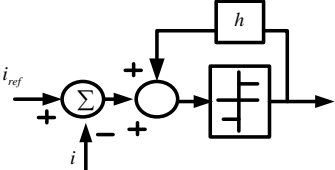


Figure 2.15: Hysteresis current controller

Chapter 3

PARAMETER ESTIMATION OF THE SRM

3.1 Determination of the Inductance and Resistance Values of the Motor

Two tests are performed, in order to evaluate the inductance and the resistance. A dc test for the stator resistance and an ac test for calculating the inductance value.

The machine investigated has a construction of 6/4 which means a three phase machine with two stator windings on each phase.

A connection diagram is shown in Fig. 3.1 for measurement of the stator resistance.

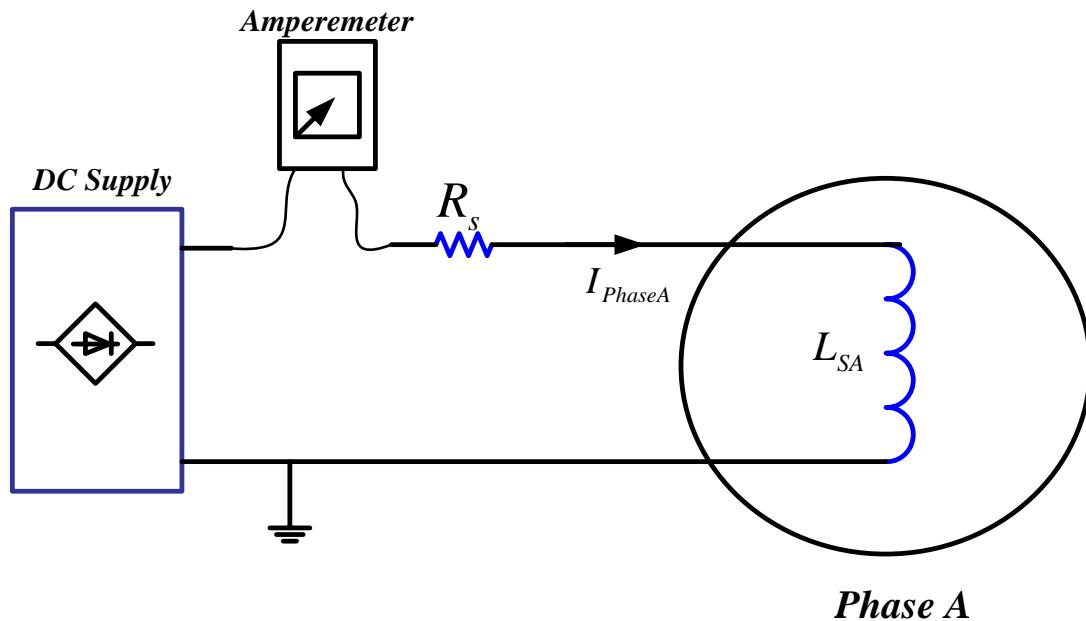


Figure 3.1: Test set-up to measure the stator resistance of a SRM

A dc voltage is applied to the stator winding of a SRM and the stator resistance can be determined using the Ohms law.

$$R_s = \frac{V_{dc}}{I_{dc}}. \quad (3.1.1)$$

The same method is performed for measurement the inductance, but instead of a dc voltage an ac voltage is applied to the SRM. Fig. 3.2 shows an ac test for the SRM.

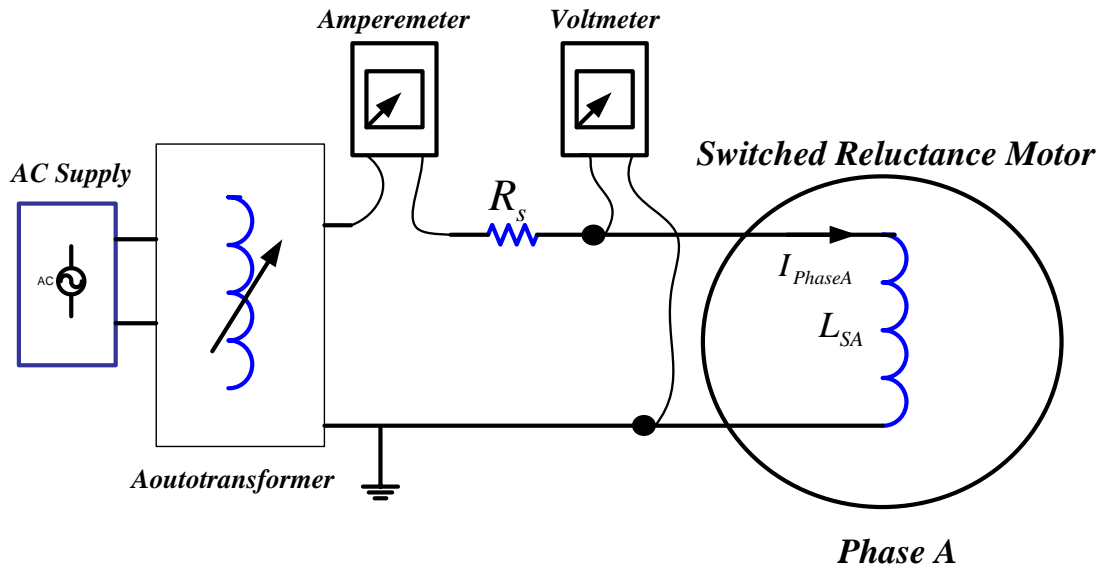


Figure 3.2: Test set-up to measure the aligned and unaligned inductances of a SRM

Usually, the range of the ratio between unaligned and aligned inductance should be according to [1],

$$0.07 < \frac{L_u}{L_a} < 0.18. \quad (3.1.2)$$

The importance of being in this range is to keep the inductance in an aligned position within an acceptable range. Since the aligned inductance is inversely proportional to the air-gap length, any decrease in the air-gap, results in an increase in the aligned inductance which prevents the DC link to maintain the current at a desired reference level.

3.2 Comparison of the Practical Measurements with Maxwell Software

As explained in Section 3.1, the minimum and maximum inductances were determined by practical tests. Then, the machine was disintegrated since it had no any manufacturer data sheet, in order to make a model in Maxwell software to do a simulation to compare the practical values of the inductances with the simulated ones. The parameters of the machine geometry are listed in the table 3.2.1.

Table 3.2.1: Parameters of the machine geometry

<i>Number of stator poles</i>	$N_s = 6$
<i>Stator outer diameter</i>	$D_{so} = 111 \text{ mm}$
<i>Stator inner diameter</i>	$D_{si} = 57 \text{ mm}$
<i>Number of rotor poles</i>	$N_r = 4$
<i>Outer rotor diameter</i>	$D_{ro} = 59 \text{ mm}$
<i>Inner rotor diameter</i>	$D_{ri} = 20 \text{ mm}$
<i>Stator yoke thickness</i>	$Y_{sth} = 12 \text{ mm}$
<i>Rotor yoke thickness</i>	$Y_{rth} = 10 \text{ mm}$
<i>Air gap length</i>	$l_{airgap} = 0.28 \text{ mm}$
<i>Stator pole angle</i>	$\beta_s = 30^\circ$
<i>Rotor pole angle</i>	$\beta_r = 32^\circ$
<i>Number of turns</i>	$N_{turn} = 500$

Table 3.2.1 shows the measurement values of voltages and currents to determine unaligned and aligned inductances of the SRM.

Table 3.2.2 shows the comparison of the practical measurement and simulated ones for unaligned and aligned inductances of the SRM.

Table 3.2.1: Measurement of voltages and currents to calculate the L_a and L_u

Rotor angles	AC Voltage(V)	Current (A)	$L (\theta)$
$\theta_1 = 0^\circ$	145	1.52	303
$\theta_2 = 10^\circ$	100	1.7	187.2
$\theta_3 = 20^\circ$	60	1.8	106.1
$\theta_4 = 30^\circ$	30	1.92	49.6

Table 3.2.: Minimum and maximum inductance values, practical and simulation measurement

	<i>Practical Values</i>	<i>Simulation Values</i>
L_u	49.6 mH	58.83 mH
L_a	303 mH	294.45 mH

The simulation result in Fig. 3.3 shows the minimum and maximum inductances which are very close to the practical measurement values presented in Table 2. In addition, the geometry of the machine is also drawn by Ansys software and shown in Fig. 3.4.

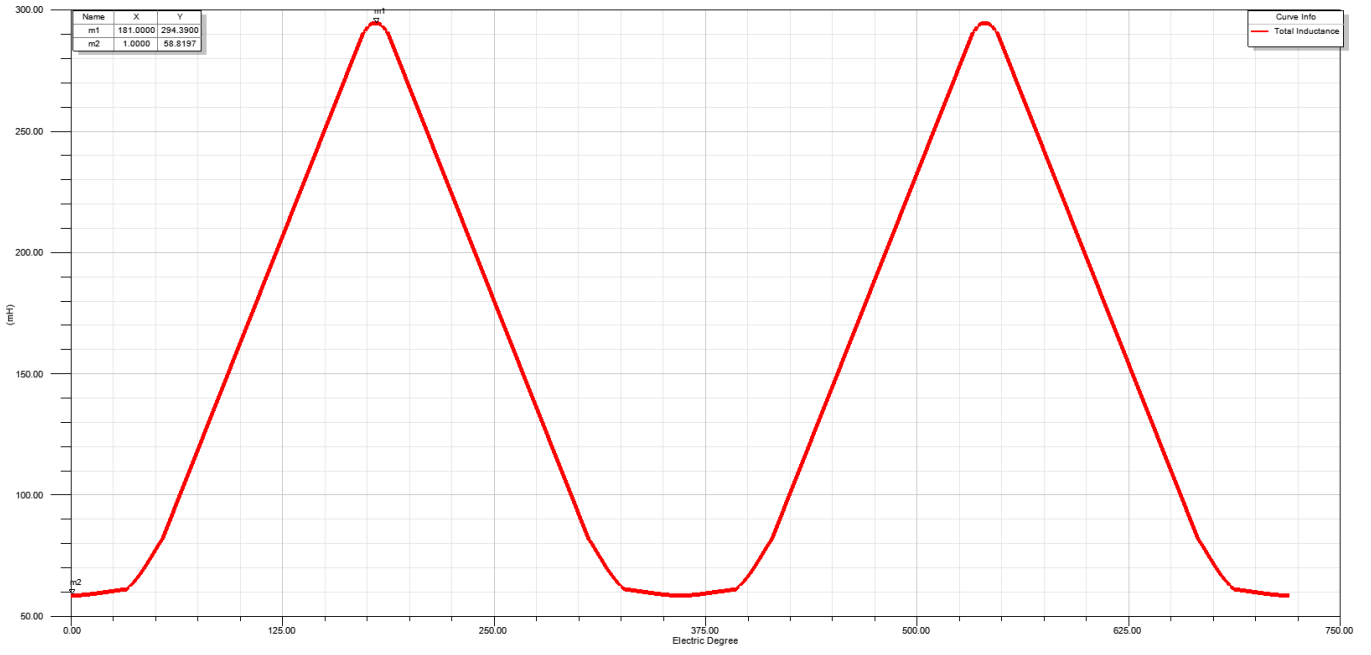


Figure 3.3: Maximum and minimum inductances simulated by the software

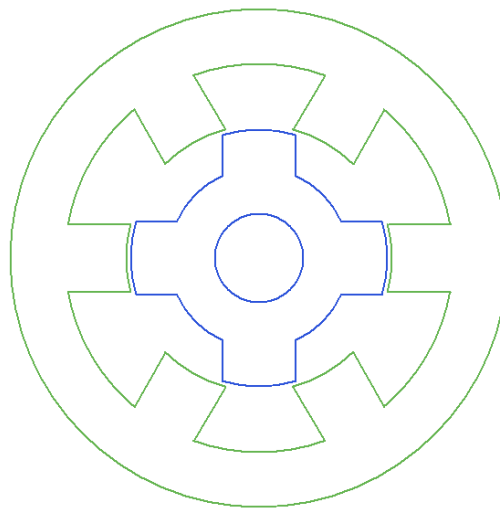


Figure 3.4: Geometry of the SRM

Chapter 4

SPEED CONTROL OF THE SWITCHED RELUCTANCE MOTOR

4.1 Mechanical Model with Friction

To control the speed of the SRM, mechanical equations for the load should be taken into account in simulation process and by this strategy the speed behavior of the motor under load and without the load would be examined.

In a mechanical model, the friction can be included in the system and the equation is as follows

$$T_{friction} = B\omega. \quad (4.1.1)$$

Using the above equation, the motion equation of a rotating system is expressed as follows

$$T_e = J_{eq} \frac{d\omega_m}{dt} + B\omega + T_L. \quad (4.1.2)$$

where T_e is the electromagnetic torque for the motor.

The graphical figure shows when the motor aims to drive the load based on the equations above;

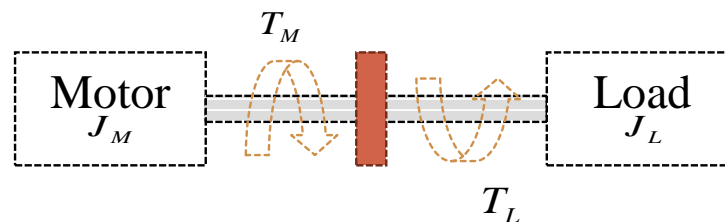


Figure 4.1: Mechanical drive of the motor system

4.2. Matlab/ Simulink Simulation of Speed Control

. The schematic structure of the speed closed -loop controller is shown in Fig. 4.2.

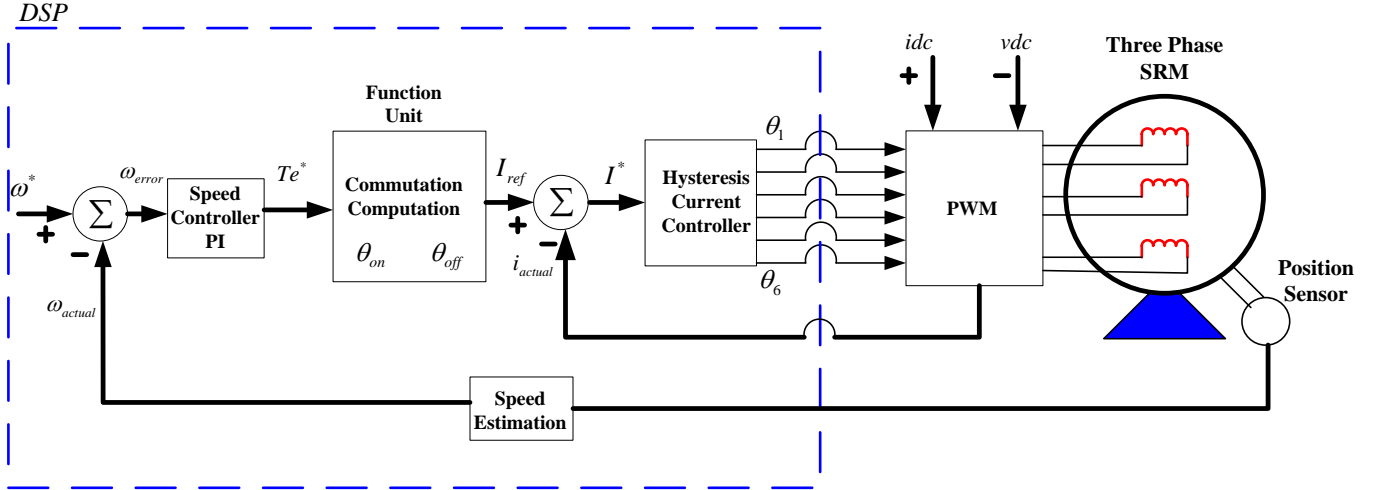


Figure 4.2: The main diagram of the speed control of a SRM

The function unit calculates the turning on θ_{on} and turning off θ_{off} angles. In this unit, torque, current and angles are the input of the function. Each phase is energized according to the command values. It is very important to calculate the turning on θ_{on} angle, in order to produce the torque. This is explained in Chapter 2 as torque is a function of the current and inductance. If the voltage drop across the stator resistance is neglected, then the turning on θ_{on} angle can be calculated as follows;

$$\theta_{on} = L_u \frac{i_{desired}}{u_{phase}} \omega_{actual} \quad (4.1.4)$$

where:

$i_{desired}$: Desired current to be achieved.

L_u : Unaligned inductance.

u_{phase} : Applied phase voltage.

ω_{actual} : Actual rotor speed.

4.3. PI Speed Controller with an Anti-Wind up

In order to have a better performance of speed response i.e. lower overshoot, a reduced steady state error, faster time response, a *PI* controller with an anti-wind up is employed as a speed controller.

The input of the speed controller is the error between the speed of the motor and the reference speed. The output of the controller is the torque and the current command which in turn is the input of the current hysteresis comparator.

Fig. 4.3 shows the structure of the *PI* controller with an anti-wind up, the gain and saturation blocks.

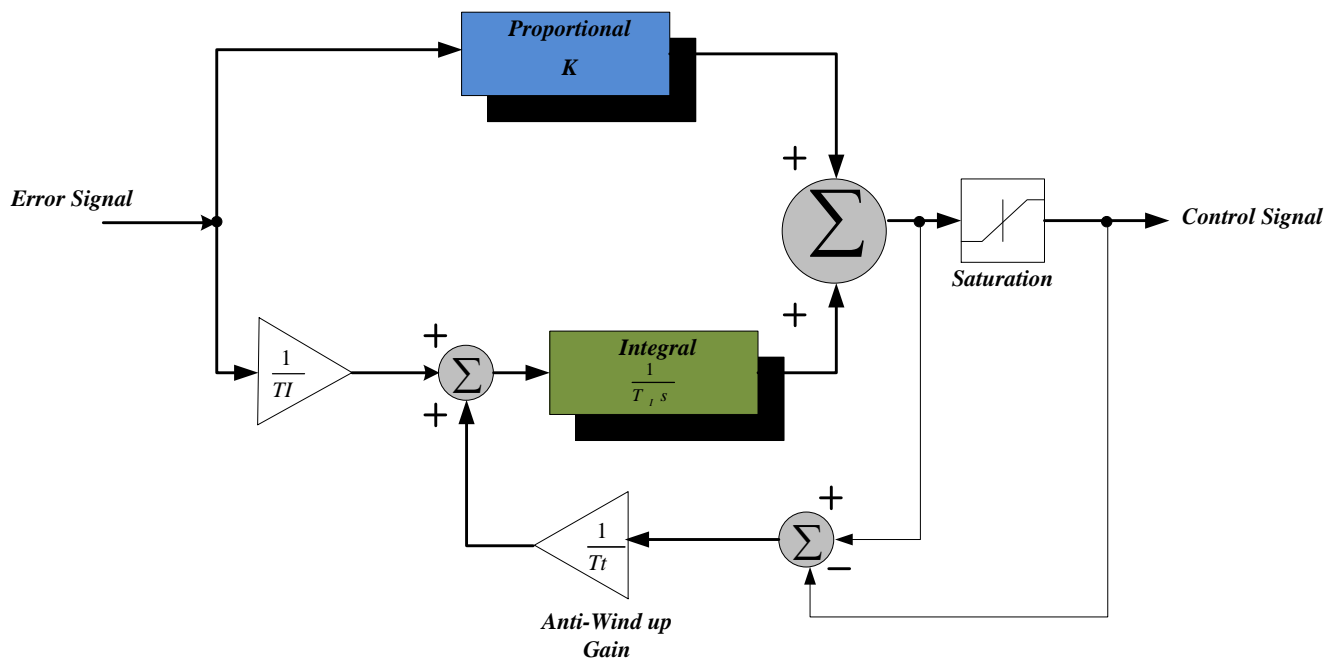


Figure 4.3: PI controller with an anti-wind up

The parameters of the speed controller K_p and K_i are determined from the following equations [2]:

$$-\frac{K_i \cdot K_t}{J \cdot (\omega_{c-w})^2} = \cos(\phi_{pm} - 180^\circ). \quad (4.1.5)$$

$$-\frac{K_p \cdot K_t}{J \cdot (\omega_{c-w})} = \sin(\phi_{pm} - 180^\circ). \quad (4.1.6)$$

where

$$\omega_{c-w} = 2\pi \cdot f_{c-w} [\text{rad}/s]. \quad (4.1.7)$$

$$K_t = \frac{T_{em}}{I} [N.m/A]. \quad (4.1.8)$$

For a crossover frequency f_{c-w} smaller than the *PWM* switching frequency and a phase margin in this range $45^\circ \leq \phi_{pm} \leq 90^\circ$, the system is stable [17].

Then, K_p and K_i is used in Simulink for the closed loop speed control of the SRM.

Following Simulink blocks of SRM are presented in Fig. 4.4 and 4.5 respectively. In Fig 4.4 the actual speed is compared with the speed command. The error is fixed by the speed controller and the current and torque are the outputs which are controlled by the function units for each phase and are compared with the actual current values of the motor to control the speed.

Fig. 4.5 shows inside of phase A control block of *SRM* in which the current and torque are computed for obtaining the total electromagnetic torque of the machine.

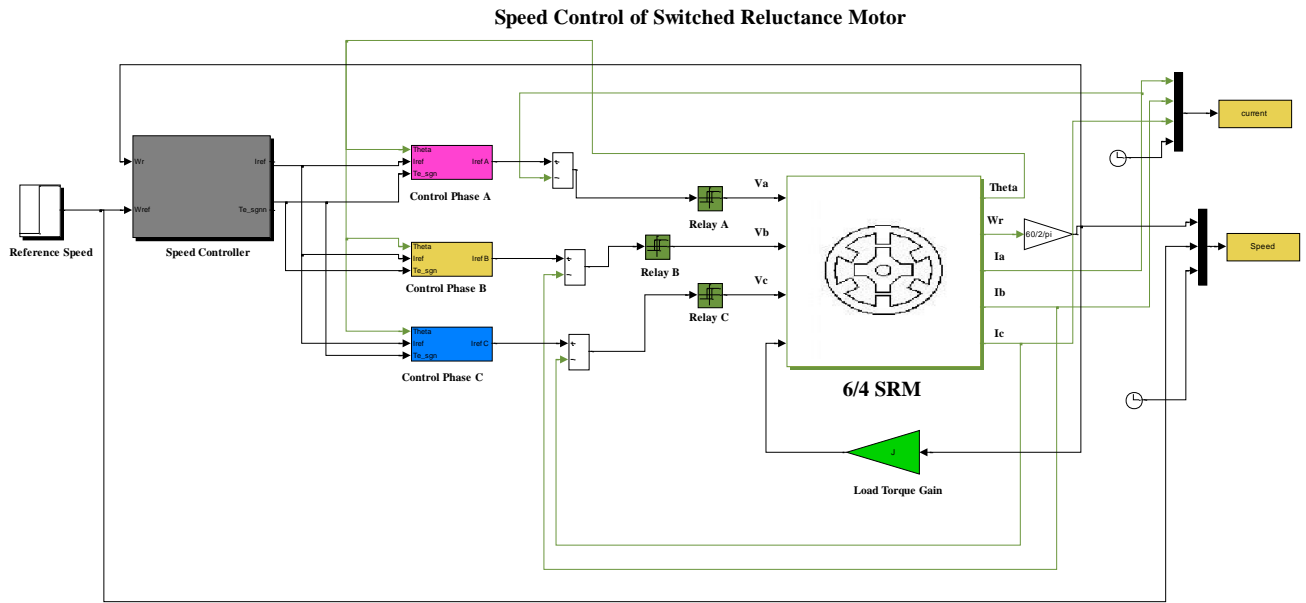


Figure 4.4: Simulink block of the Speed control of the SRM

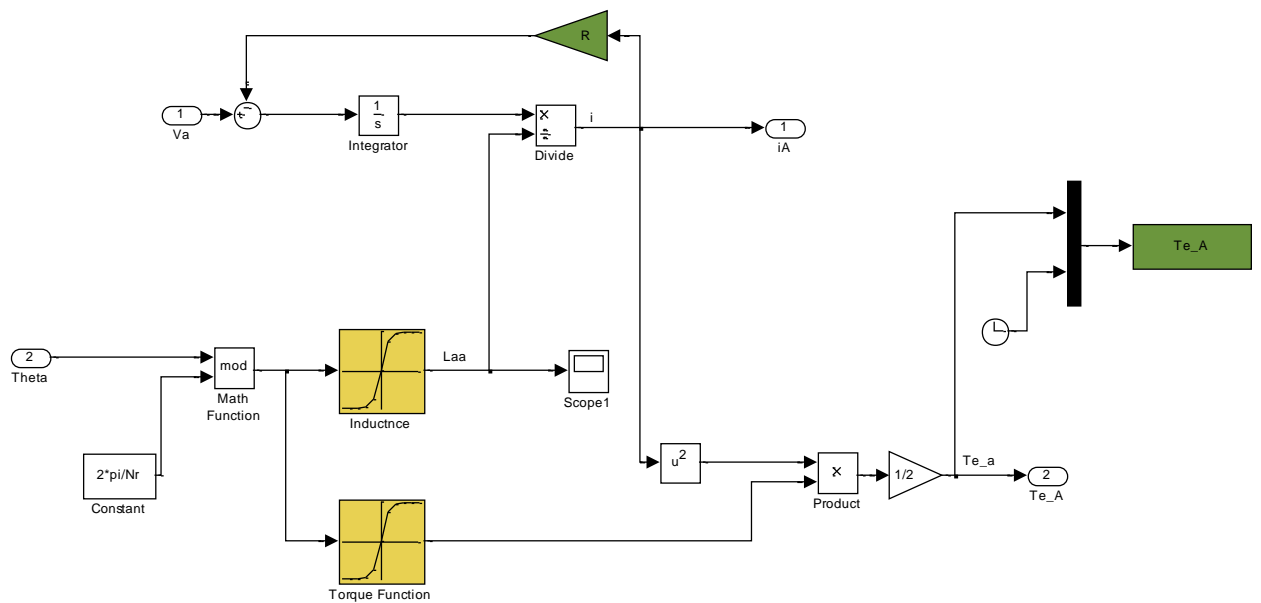


Figure 4.5: Controlling of Phase A

4.4. Simulation Results

Table 4.4.1 shows the parameters of the motor applied in Matlab/ Simulink model.

Table 4.4.1: Motor Parameters used in Simulink Model

<i>Rated Power</i>	2 KW
<i>Operation Torque</i>	19 N.m
<i>Operation Speed</i>	1000 rpm
<i>Number of Phases</i>	$m = 3$
<i>Number of Stator Poles</i>	$N_s = 6$
<i>Number of Rotor Poles</i>	$N_r = 4$
<i>Aligned Phase Inductance</i>	$L_a = 300\text{mH}$
<i>Unaligned Phase Inductance</i>	$L_u = 50\text{mH}$
<i>Inertia</i>	$J = 0.0088\text{Kg.m}$
<i>Resistance</i>	$R = 0.95\Omega$
<i>DC Voltage Supply</i>	$V_{dc} = 300\text{V}$

Following simulation tests are performed to investigate the ability of the speed controller. First, the motor is simulated without the effect of the load by a step input to examine the accuracy of the controller. The operation speed of the motor is assumed to be 1000 rpm . Fig.4.6 illustrates the transient speed response that meets the requirement as can be seen, it is stable after reaching the reference value.

Fig. 4.7 illustrates the simulated transient speed response when a load 4 N.m is applied. The motor speed can track the speed command well and the effect of the load application produces some oscillations in this case.

Fig. 4.8 and 4.9 are the magnified view of the speed control for no load and loaded operating condition respectively. It can be seen that the speed controller controls the speed of the SRM well, but in both cases the effect of the oscillation is visible and this is one of the disadvantages of the SRM.

To make sure that speed controller has the flexibility to regulate the actual speed under sudden disturbances, two cases are studied. One for load application from stand still 4 N.m and changing to 1 N.m during the time interval 1 (s) and 1.2 (s) and the other from stand still 1 N.m and changing to 4 N.m during the time interval 1 (s) and 1.2 (s)

Fig. 4.10 shows the variation of the actual speed under above circumstances. When the rated load 4 N.m is applied from standstill speed controller controls the actual speed until the load is changed to 1 N.m which means decreasing load and resulting in a speed increase and immediately the speed controller adjusts the actual speed to reach the speed command.

Fig. 4.11 shows the variation of the actual speed under a load disturbance. In this case a load of 1 N.m is applied from standstill and changes to the rated load 4 N.m which means increasing load and it results in a speed decrease and immediately the speed controller regulates the actual speed to reach the speed command. Fig. 4.12 and 4.13 are the magnified views of these results.

In previous tasks, the speed controller is used only for the motoring operation condition and in order to realize that it can also control the actual speed in generating mode, the step input is changed from the rated speed 1000 rpm to -1000 rpm . Fig. 4.14 and 4.15 show the operation of the speed controller in four quadrants with and without the effect of the load. It can be seen that the actual speed tracks the speed command well. Fig 4.16 and 4.17 are the magnified view of the four quadrant operation respectively.

Other kinds of speed commands are used with and without the effect of the load and the behavior of the speed controller are examined in Fig. 4.18 and 4.19.

Fig. 4.20 and 4.21 are the magnified views of the speed track.

Fig. 4.21 to 4.28 show the phase currents, torques, total phase currents and total electromagnetic torque produced by the motor respectively. During the load application, motor starts to draw current and torque is produced to drive the rated load.

As mentioned earlier, when the hysteresis current control method is used to control the motor currents, it produces more pulsations in current waveforms due to the effect of the fast switching frequency. This method is used for low and middle speeds, because there is enough time to control the phase currents.

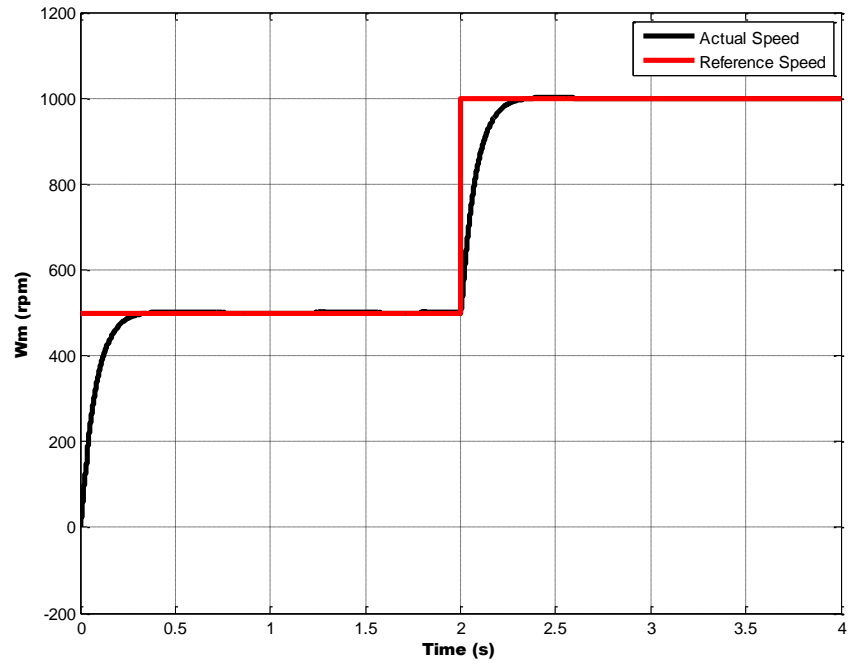


Figure 4.6: Motor speed and speed command without the load effect

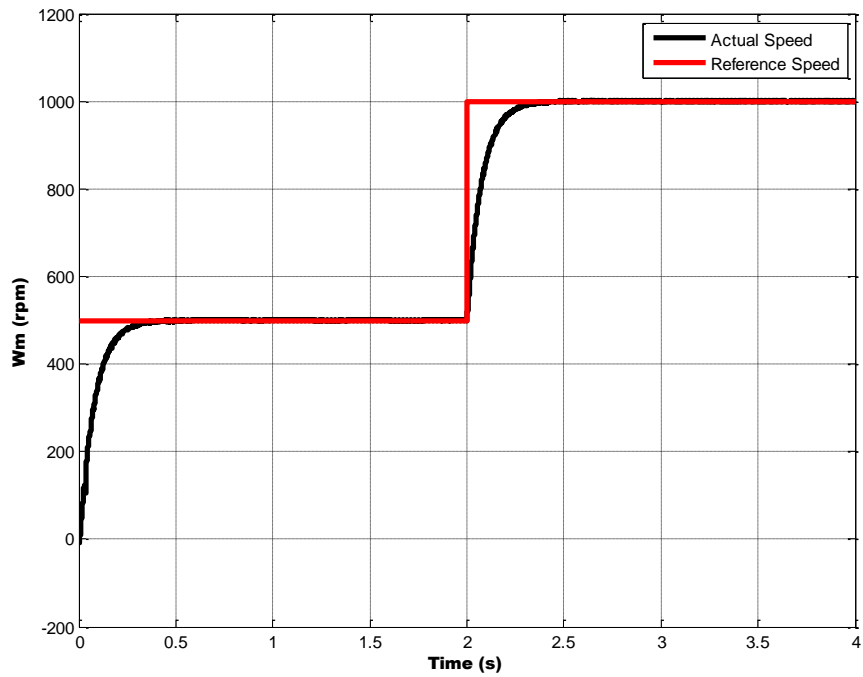


Figure 4.7: Motor speed and speed command with the load effect

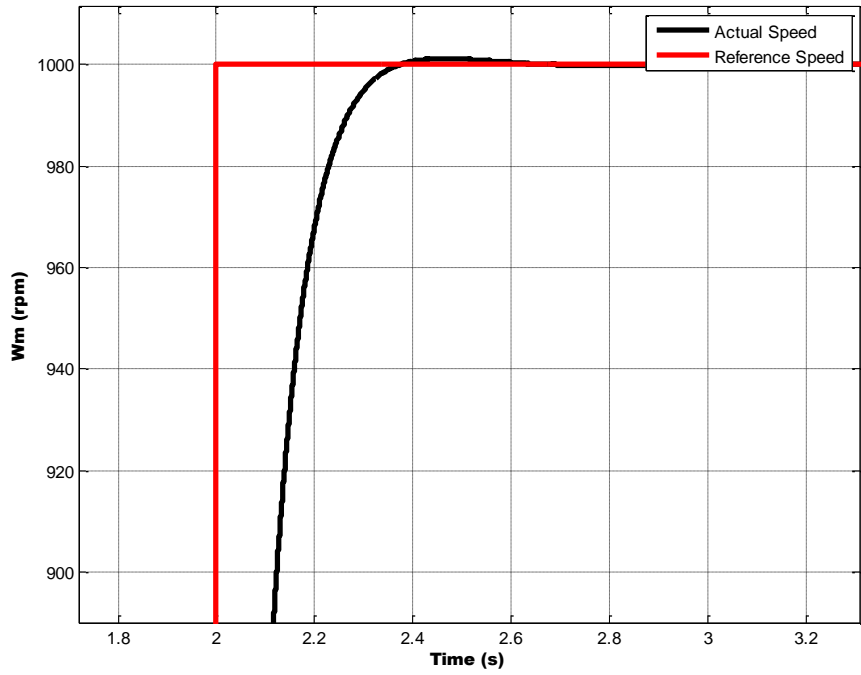


Figure 4.8: Magnified motor speed and speed command without the load effect

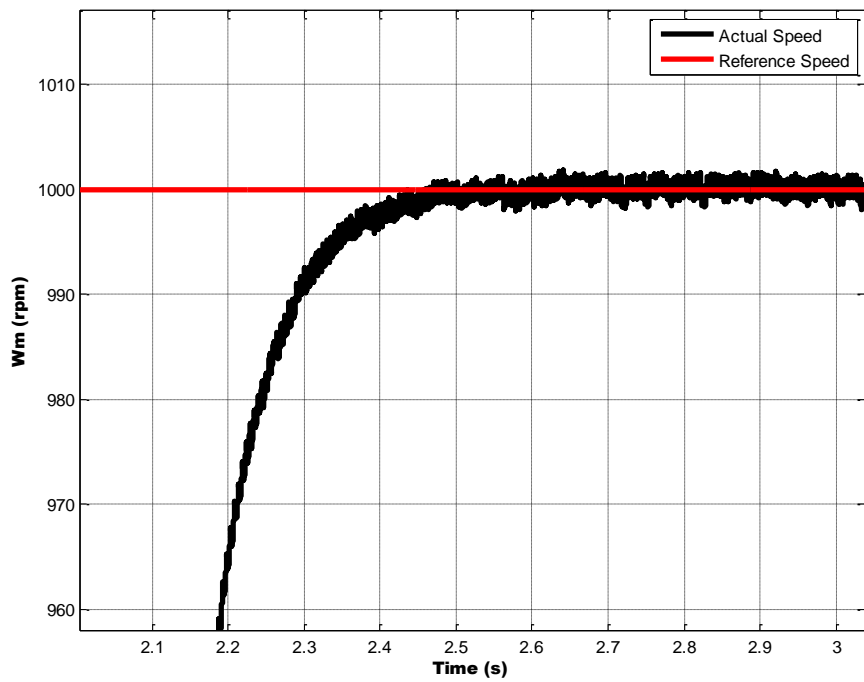


Figure 4.9: Magnified motor speed and speed command with the load effect

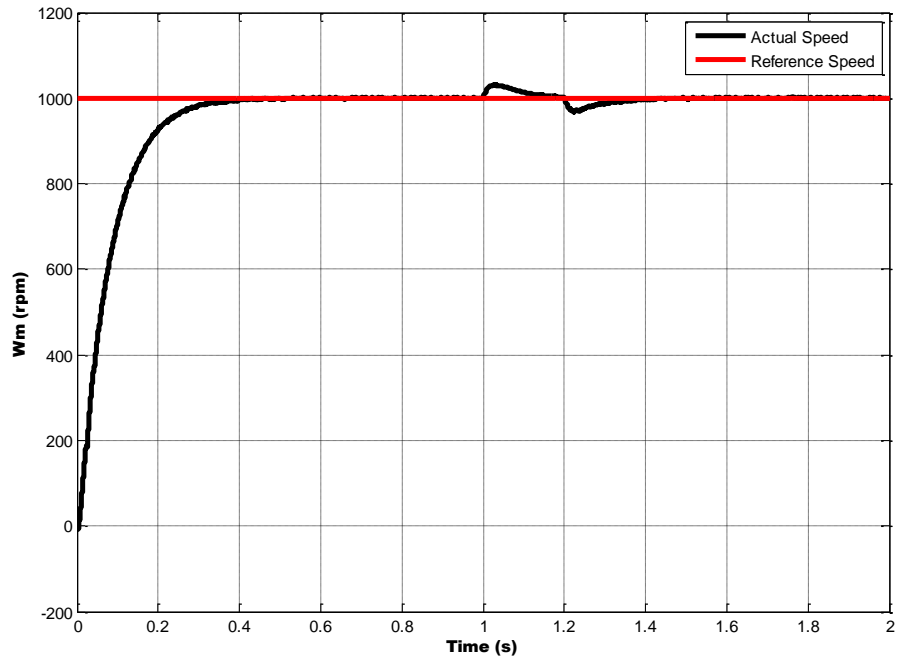


Figure 4.10: Motor speed and speed command with the load effect during a time interval

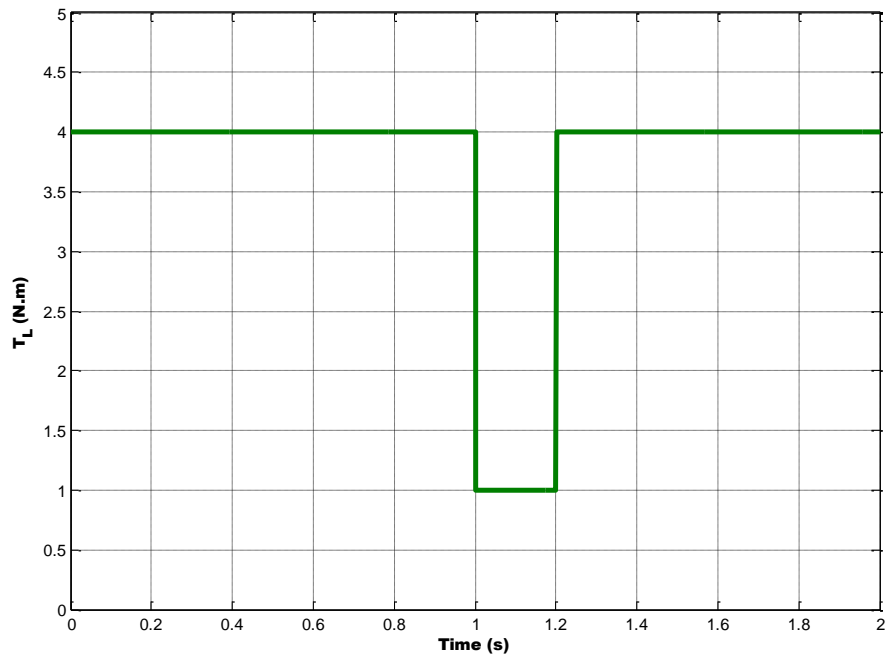


Figure 4.11: Changing the load torque during a time interval from 4 to 1N.m

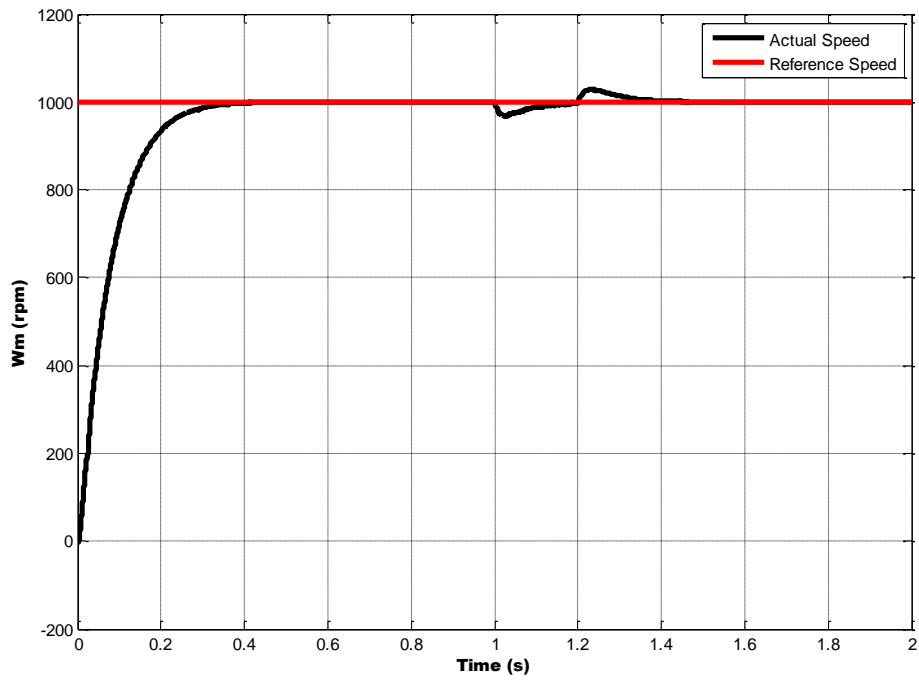


Figure 4.12: Motor speed and speed command with the load effect during a time interval

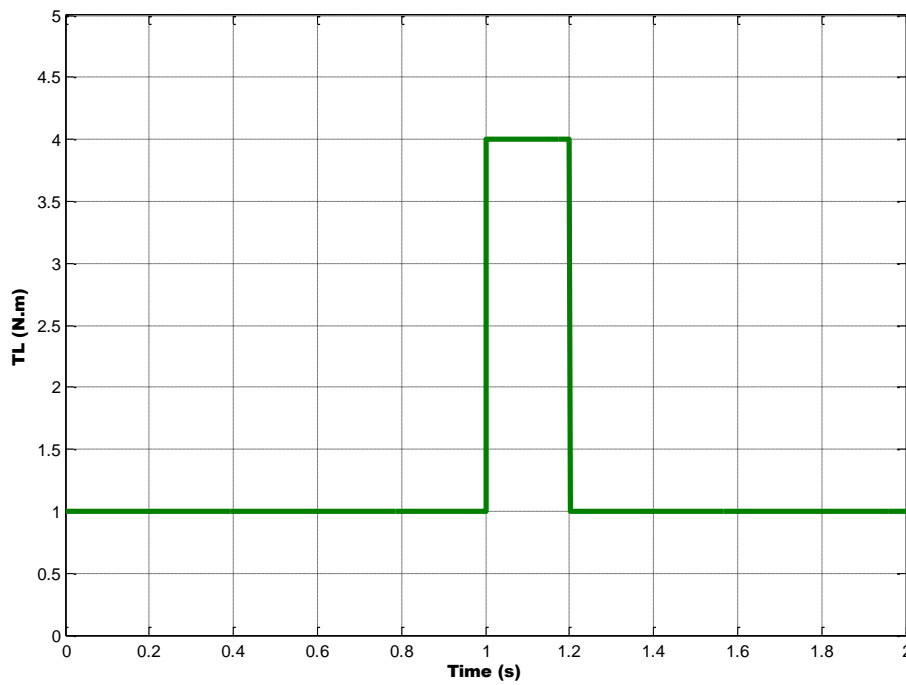


Figure 4.13: Changing the load torque during a time interval from 1 to 4N.m

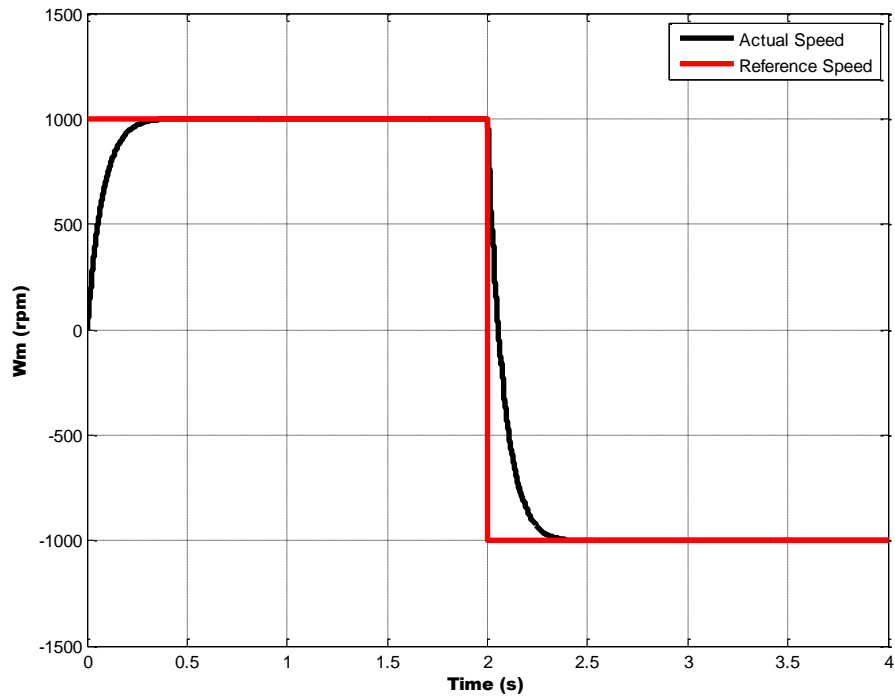


Figure 4.14: Motor speed and speed command without the load effect four quadrants

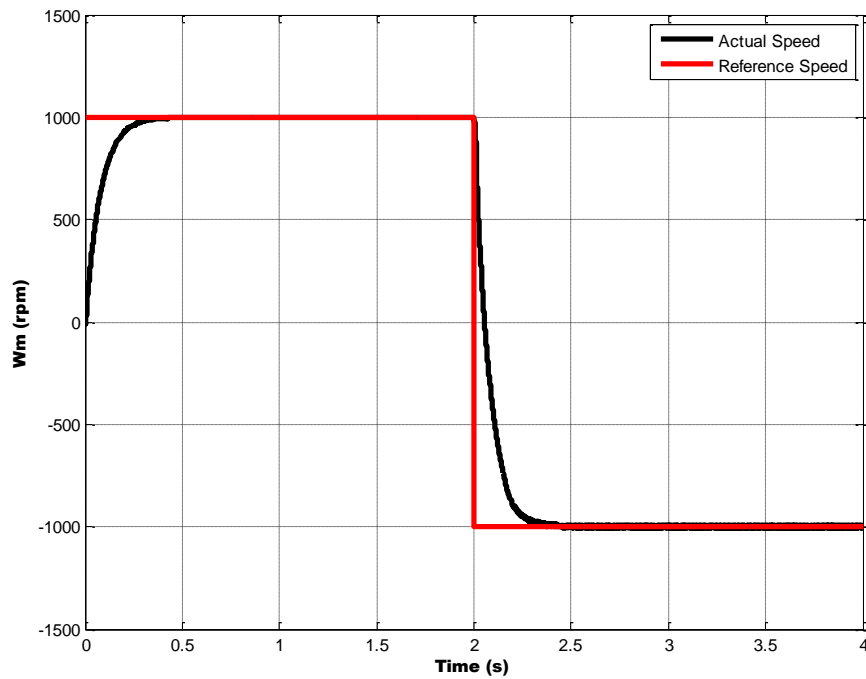


Figure 4.15: Motor speed and speed command with the load effect four quadrants

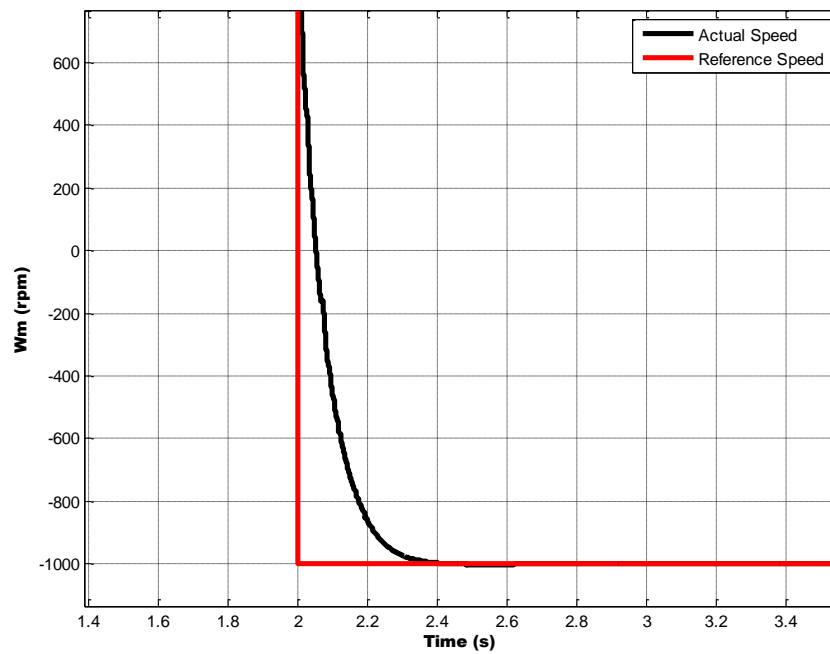


Figure 4.16: Magnified motor speed and speed command without the load effect four quadrants

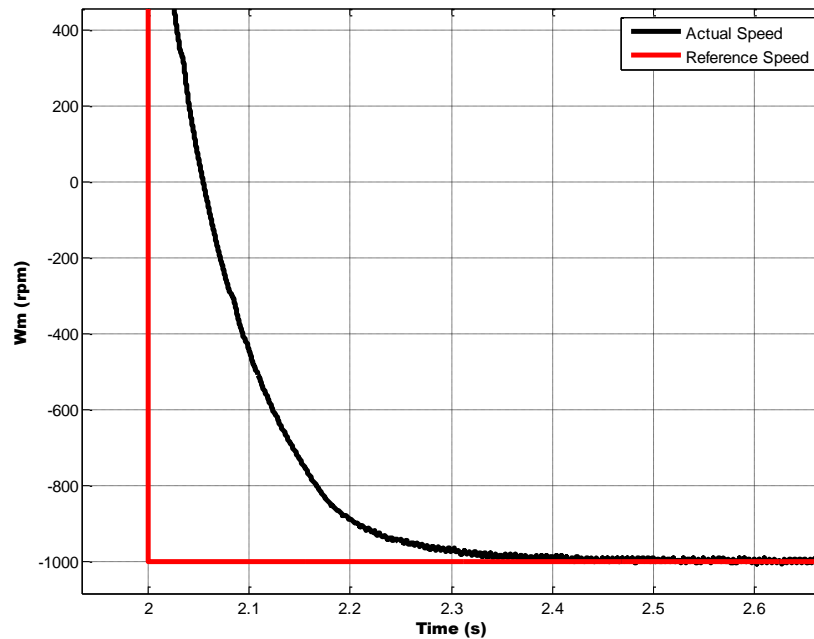


Figure 4.17: Magnified motor speed and speed command with the load effect four quadrants

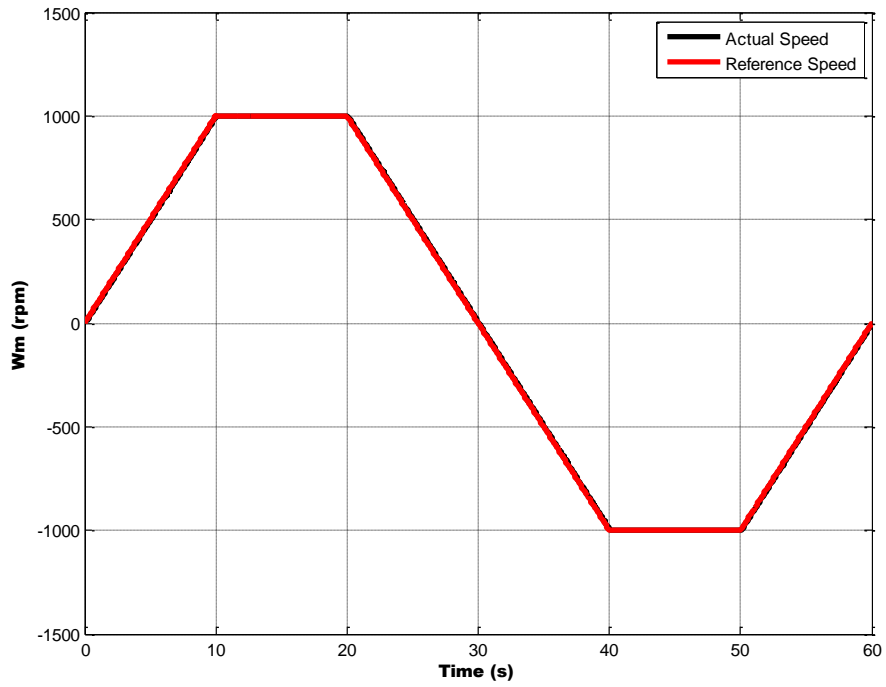


Figure 4.18: Motor speed and speed command without the load effect four quadrants

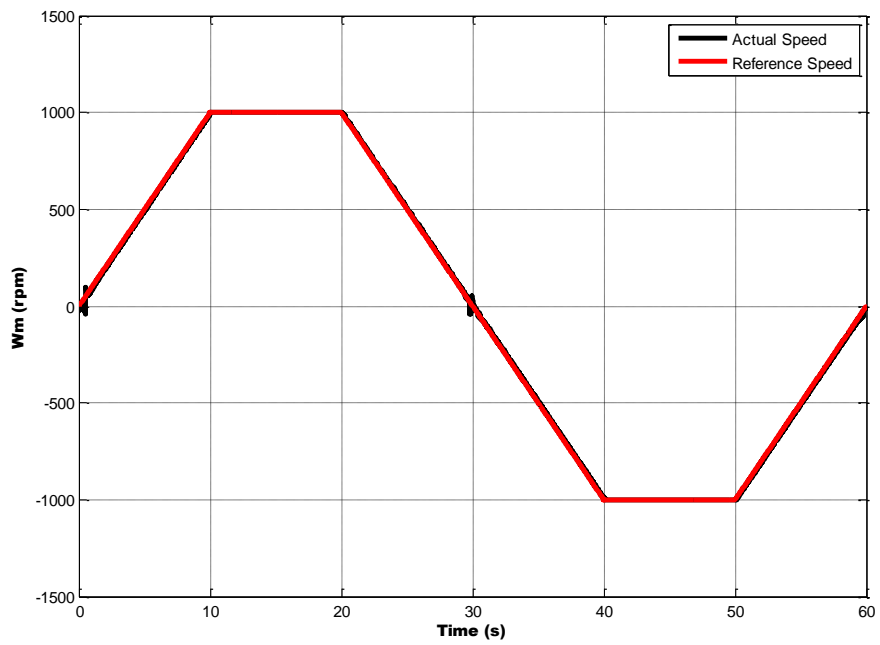


Figure 4.19: Motor speed and speed command with the load effect four quadrants

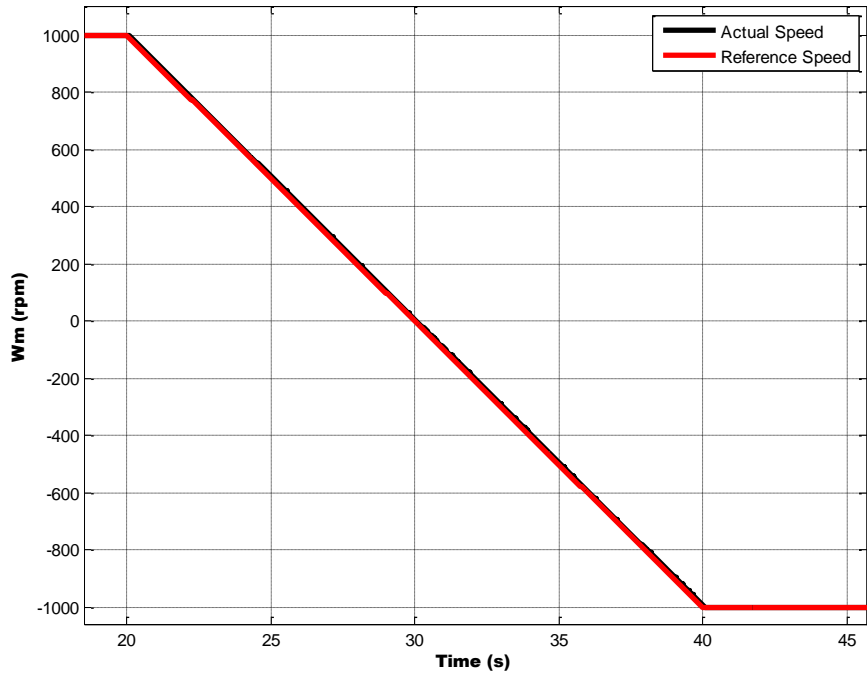


Figure 4.20: Magnified motor speed and speed command without the load effect four quadrants

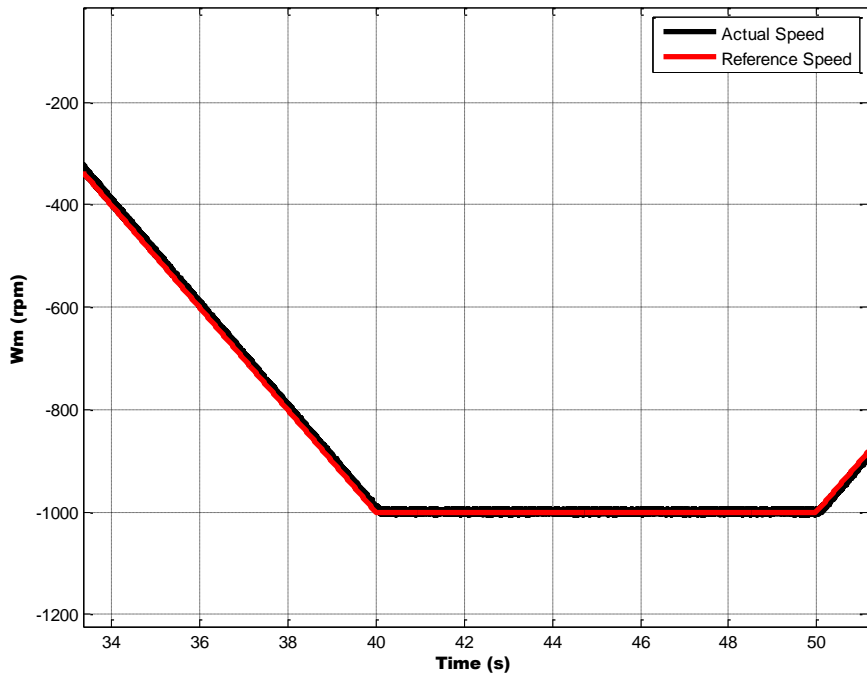


Figure 4.21: Magnified motor speed and speed command with the load effect four quadrants

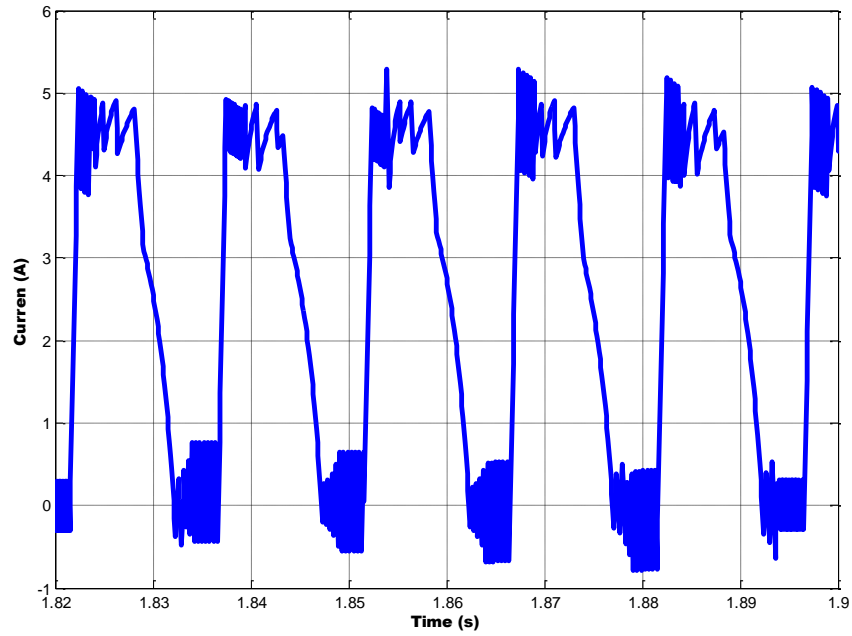


Figure 4.22: Current in phase A with the load effect at speed of 1000 rpm

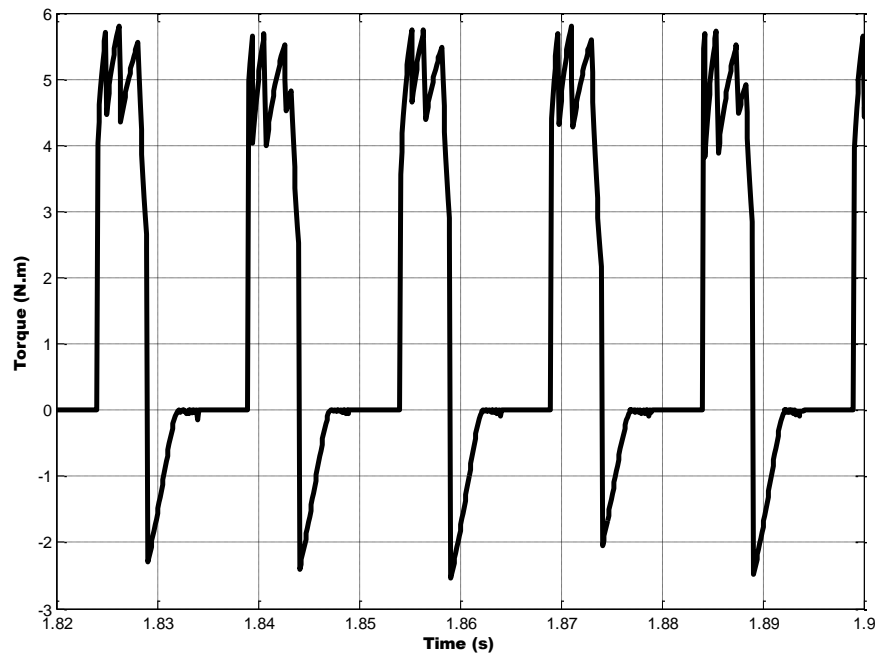


Figure 4.23: Torque in phase A with the load effect at speed of 1000 rpm

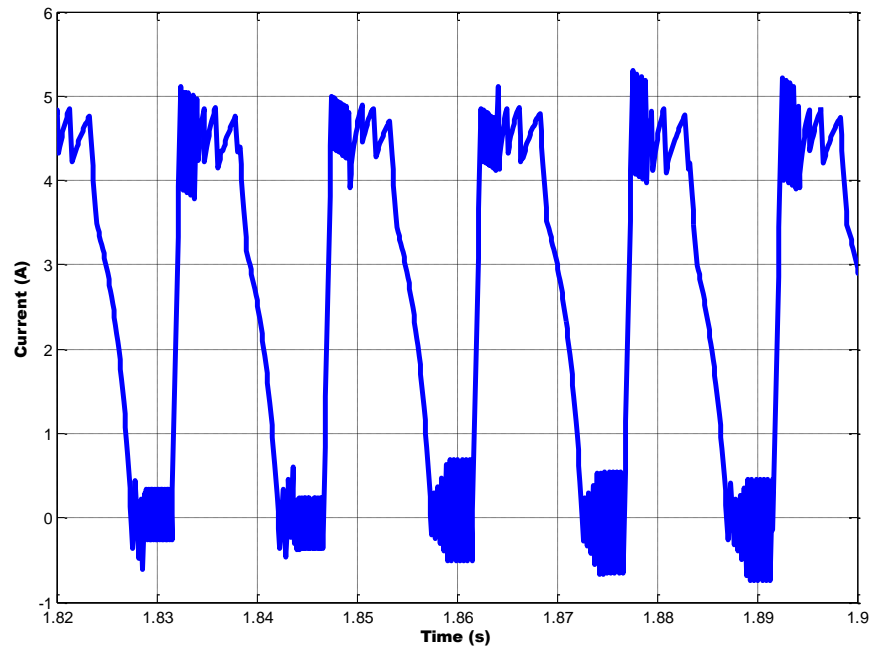


Figure 4.24: Current in phase B with the load effect at speed of 1000 rpm

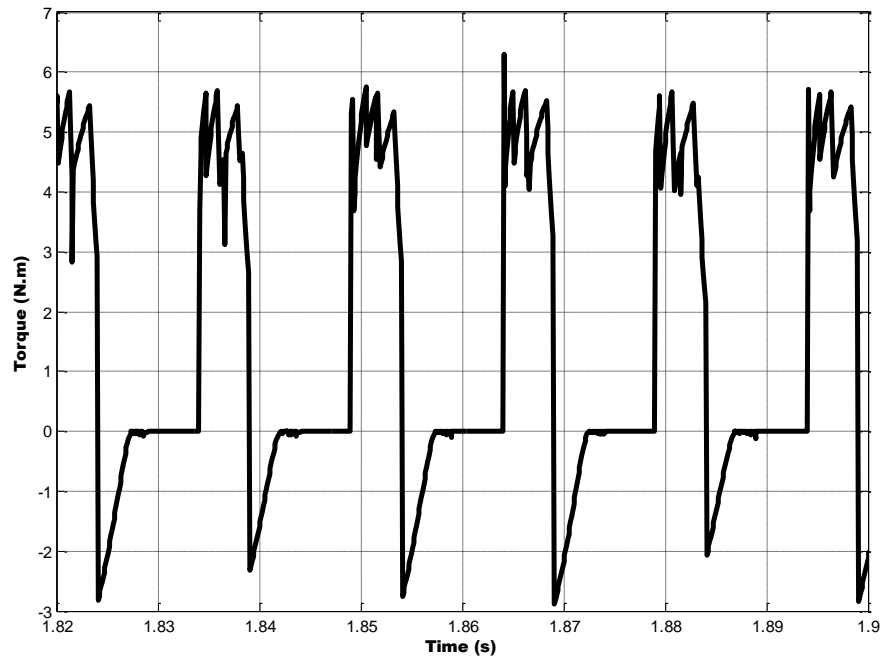


Figure 4.25: Torque in phase B with the load effect at speed of 1000 rpm

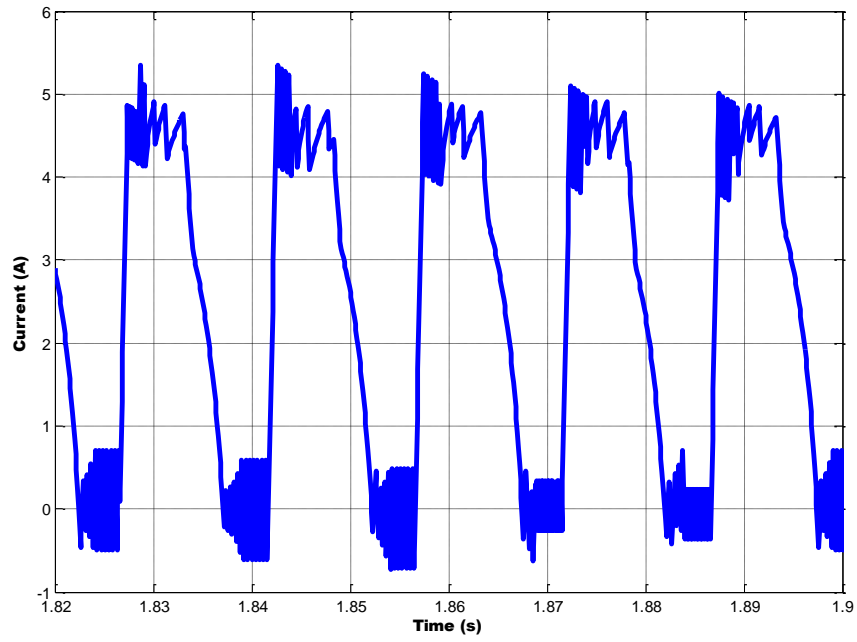


Figure 4.26: Current in phase C with the load effect at speed of 1000 rpm

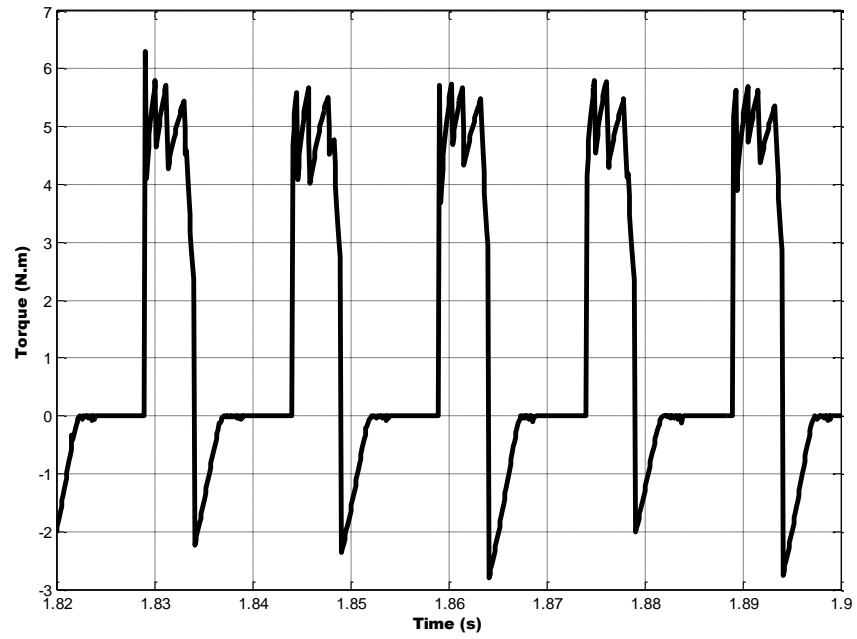


Figure 4.27: Torque in phase C with the load effect at speed of 1000 rpm

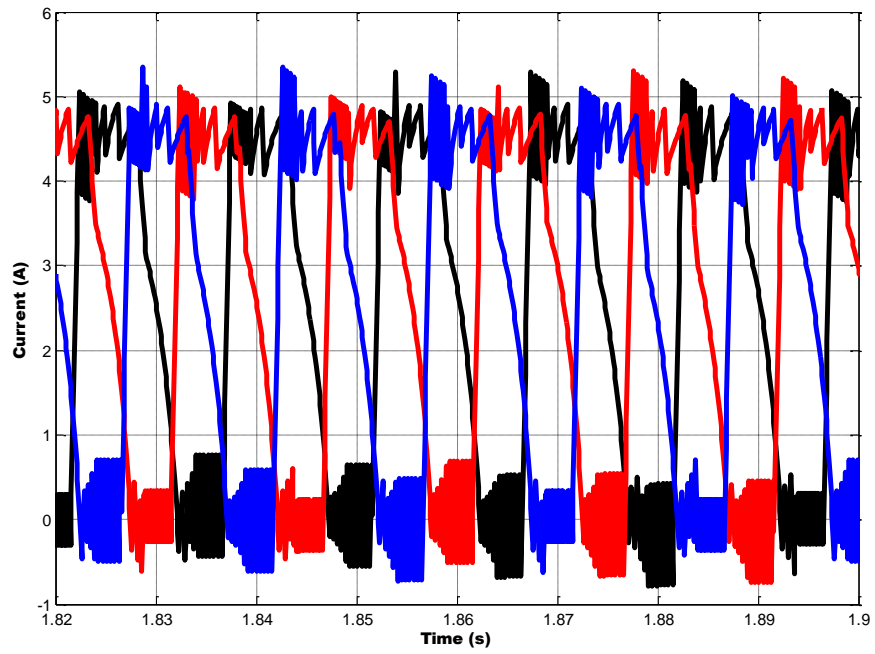


Figure 4.28: Three phase currents A, B, C with the load effect at speed of 1000 rpm

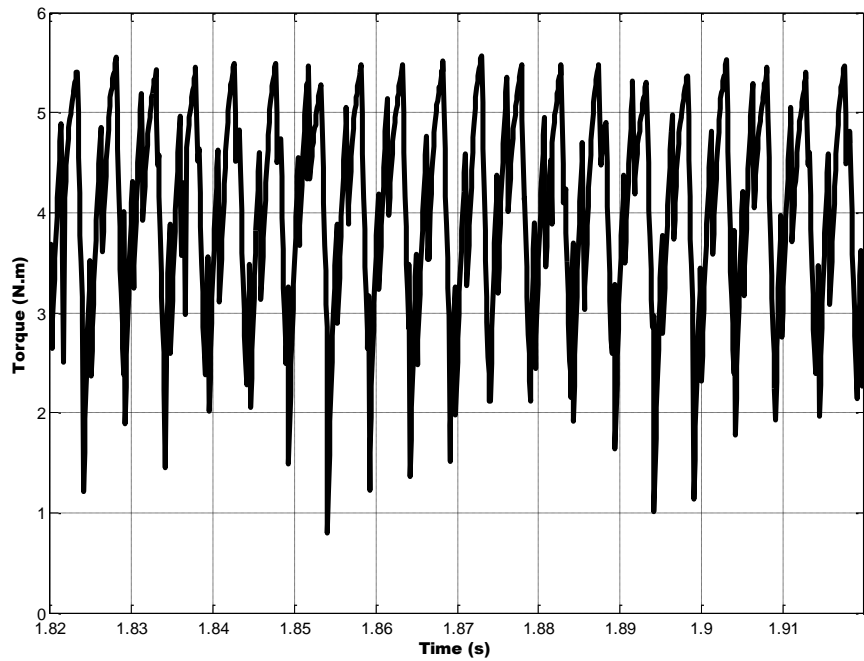


Figure 4.29: Total electromagnetic torque A, B, C with the load effect at speed of 1000 rpm

Chapter 5

EXPERIMENTAL SETUP

5.1 SRM Setup Installation

It is intended to build an experimental setup consisting of a SRM, a load, torque and encoder sensor. Fig 5.1 shows the whole system.

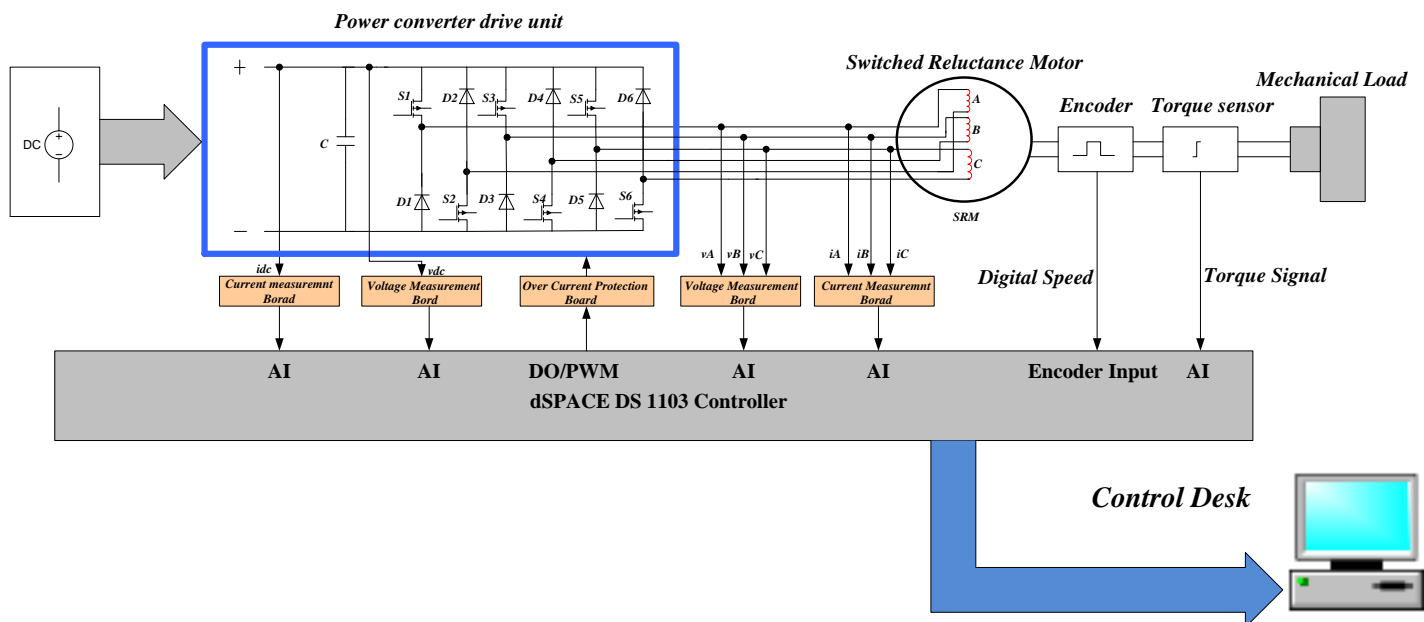


Figure 5.1: General schematic of the practical system

Fig. 5.1 above illustrates the main outline of the experimental system for the SRM drive system. The DC supply panel feeds the power converter unit for turning the MOSFET switches on and off. The SRM motor is driven from the output of the converter switches. Any phase over current is determined by the over current protection unit. In order to estimate the rotor speed and torque of the machine, an incremental encoder and a torque sensor are mounted on the motor and their signals are sent to the *dSPACE*. In total, four voltage signals, four current signals are required to be evaluated during the motor operation that is done by the voltage and current measurement units. Finally, the control algorithm is implemented in *dSPACE* system which acts as the interface between the host PC and a controller.

5.2 Hardware's Used in the Laboratory

Electrical lab instruments are listed as follows

- 1- *SRM* Motor
- 2- *DC* Source supply
- 3- Voltage, current measurement units
- 4- *dSPACE* DS1103 control system
- 5- Over current protection unit
- 6- Different electrical items such as connectors, cables and auxiliary power supply.

5.3 Switched Reluctance Motor

The specification of *SRM* used in practical implementation is described in table 5.3.1.

Table 5.3.1: Motor Parameters used in Simulink Model

<i>Rated Power</i>	2 KW
<i>Operation Torque</i>	19 N.m
<i>Operation Speed</i>	1000 rpm
<i>Number of Phases</i>	$m = 3$
<i>Number of Stator Poles</i>	$N_s = 6$
<i>Number of Rotor Poles</i>	$N_r = 4$
<i>Aligned Phase Inductance</i>	$L_a = 300\text{mH}$
<i>Unaligned Phase Inductance</i>	$L_u = 50\text{mH}$
<i>Inertia</i>	$J = 0.0088\text{Kg.m}$
<i>Resistance</i>	$R = 1.1\Omega$
<i>DC Voltage Supply</i>	$V_{dc} = 300\text{V}$

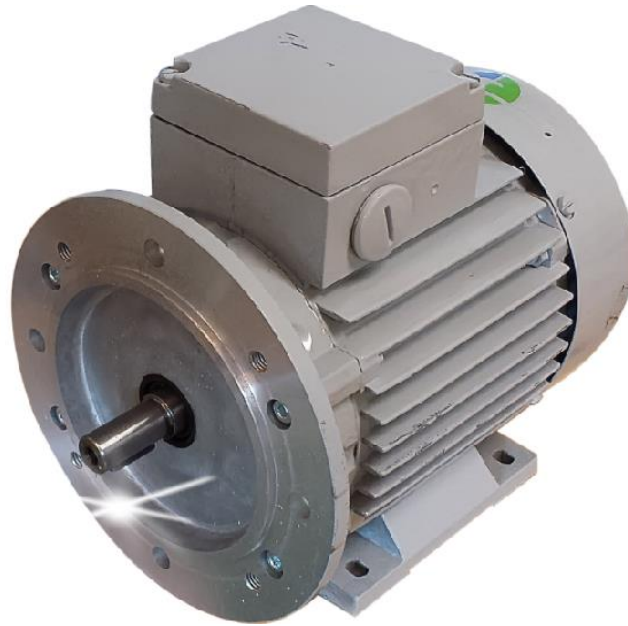


Figure 5.2: Switched Reluctance Motor *SRM*

Fig.5.2 above shows switched reluctance motor that is used in practical setup.

5.4. Power Electronic Converter

To drive the *SRM* each phase is energized independently by a power converter board. These units are the core part of a current controller. The important components of these *PCB* are *Mosefet* switches due to their high voltage rating, high current rating and fast turning on and off capability. The following pictures show the completion of the power converter units to operate the switched reluctance motor.

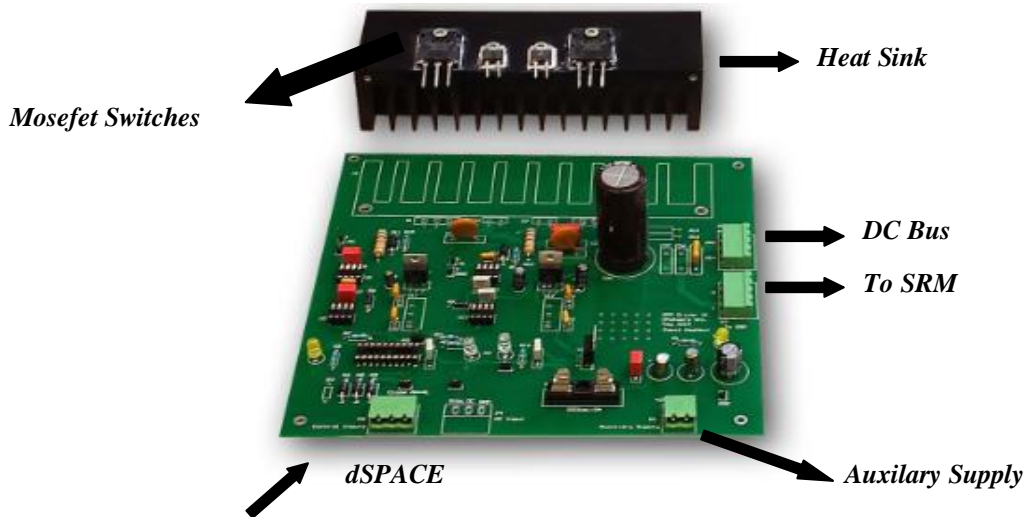


Figure 5.3: *PCB* to drive one phase of *SRM*



Figure 5.4: Three power converter boards

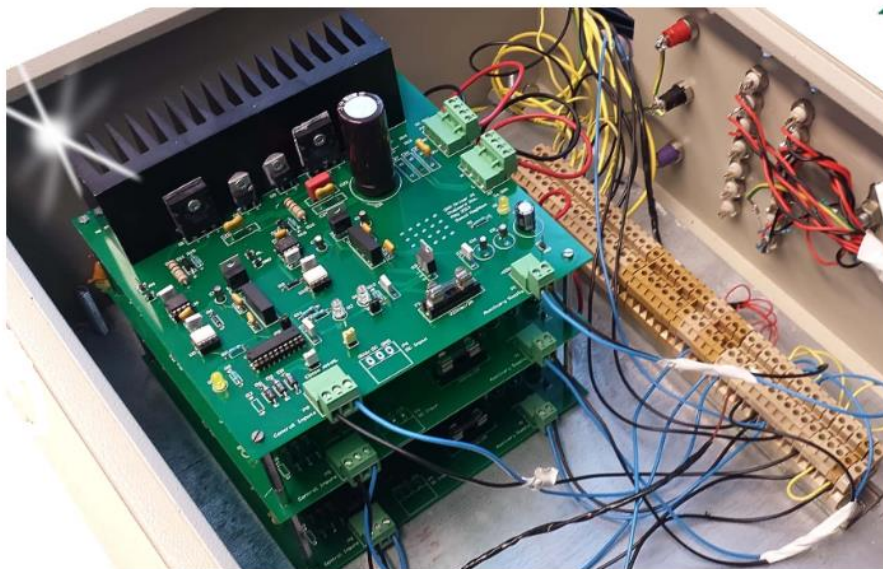


Figure 5.5: Installation of *PCB* in the box

5.5 Measurement Units of Voltages and Currents

Voltages and currents of the *DC* side are required to be measured. In order to measure the voltages, four voltage transducers *UMAT2* are used. One is used for the *DC* bus voltage and three of them are used to measure the phase voltages. They reduce the level of the actual voltage from a range $\pm 300V$ to a $\pm 10V$ signal that is used for the *dSPACE* system.

Fig.5.6 shows these voltage transducers in the measurement box unit.

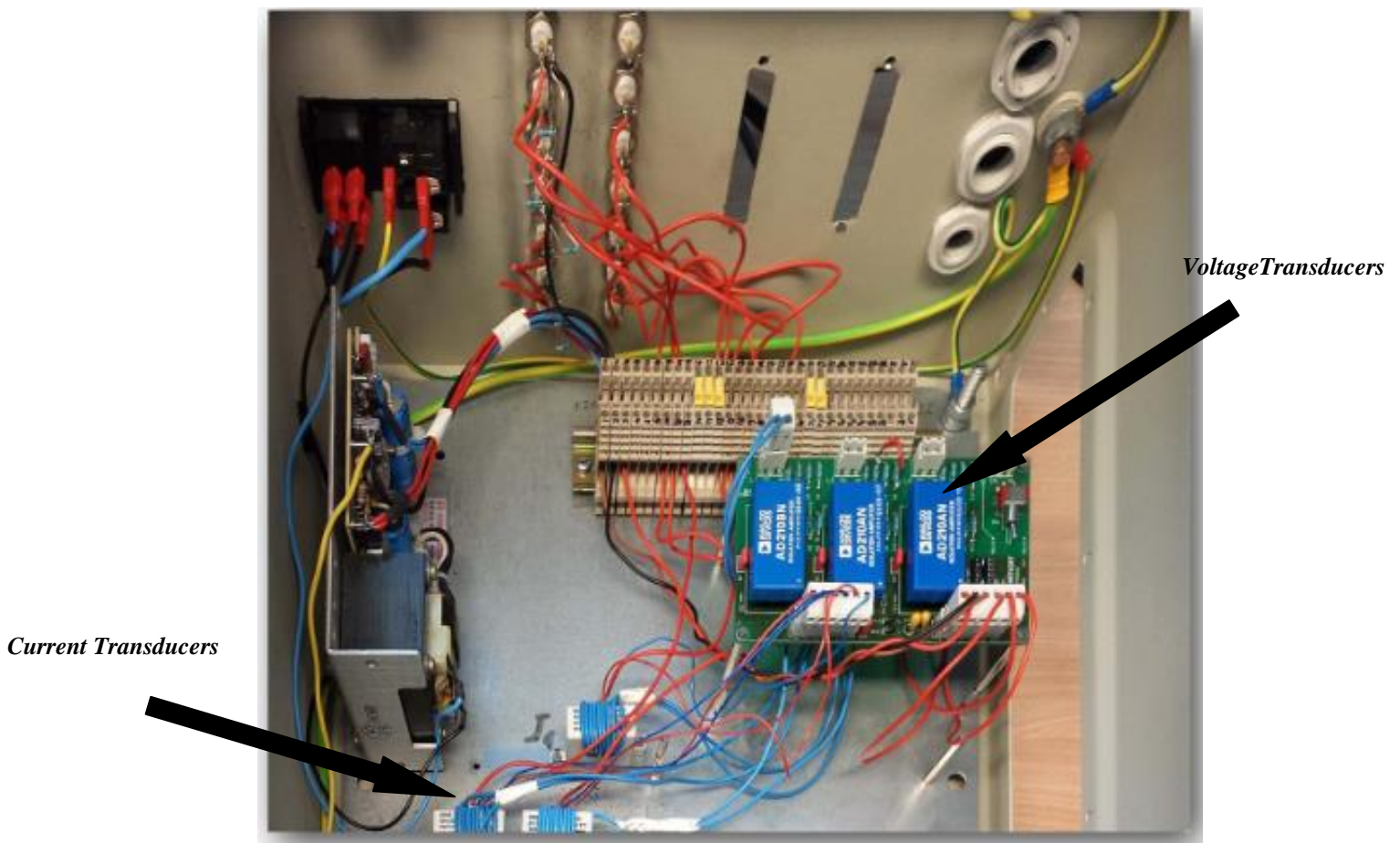


Figure.5.6: Voltage and current transducers in the measurement box unit

This is the same for the current measurements. Four current transducers *LEM LA 50-S/SP1* are used to measure the stator current of each phase of the current loop. The actual current value is reduced from a range of $10A$ to a $\pm 10V$ signal for the *dSPACE* system.

5.6 Practical Results for an Open Loop Performance

After completion of the experimental setup, currents of each phase are plotted by *dSPACE*. These currents are obtained for no load condition where switched reluctance motor only consumes electrical energy due to some losses in the windings and friction of the mechanical part.

Fig.5.7 and 5.8 show the current waveforms in phase A and the other phases.

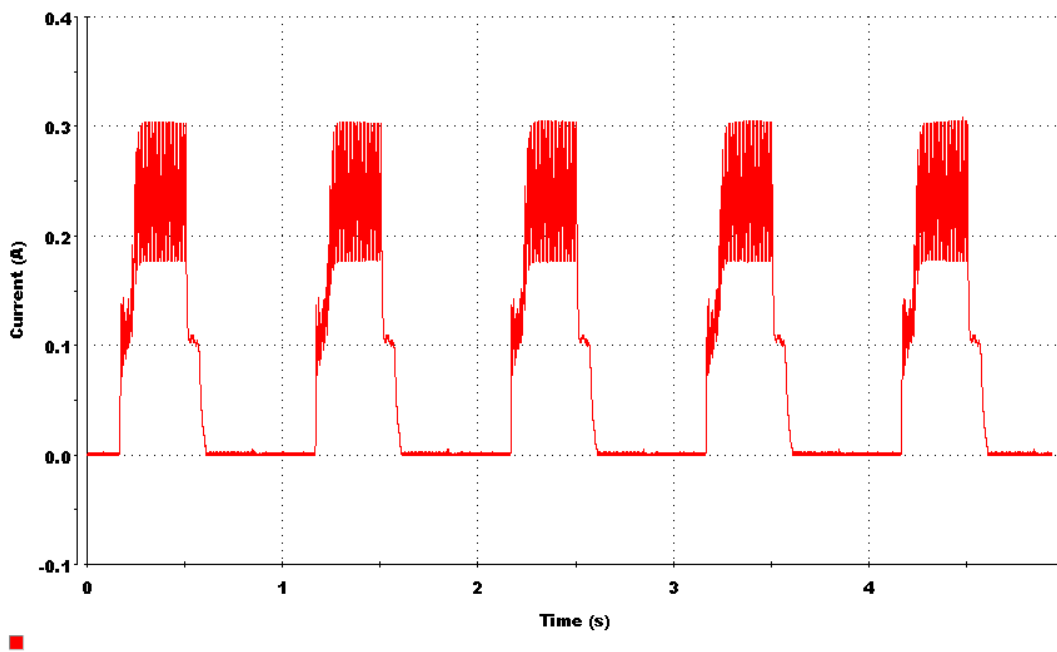


Figure.5.7: Current in phase A, open loop performance

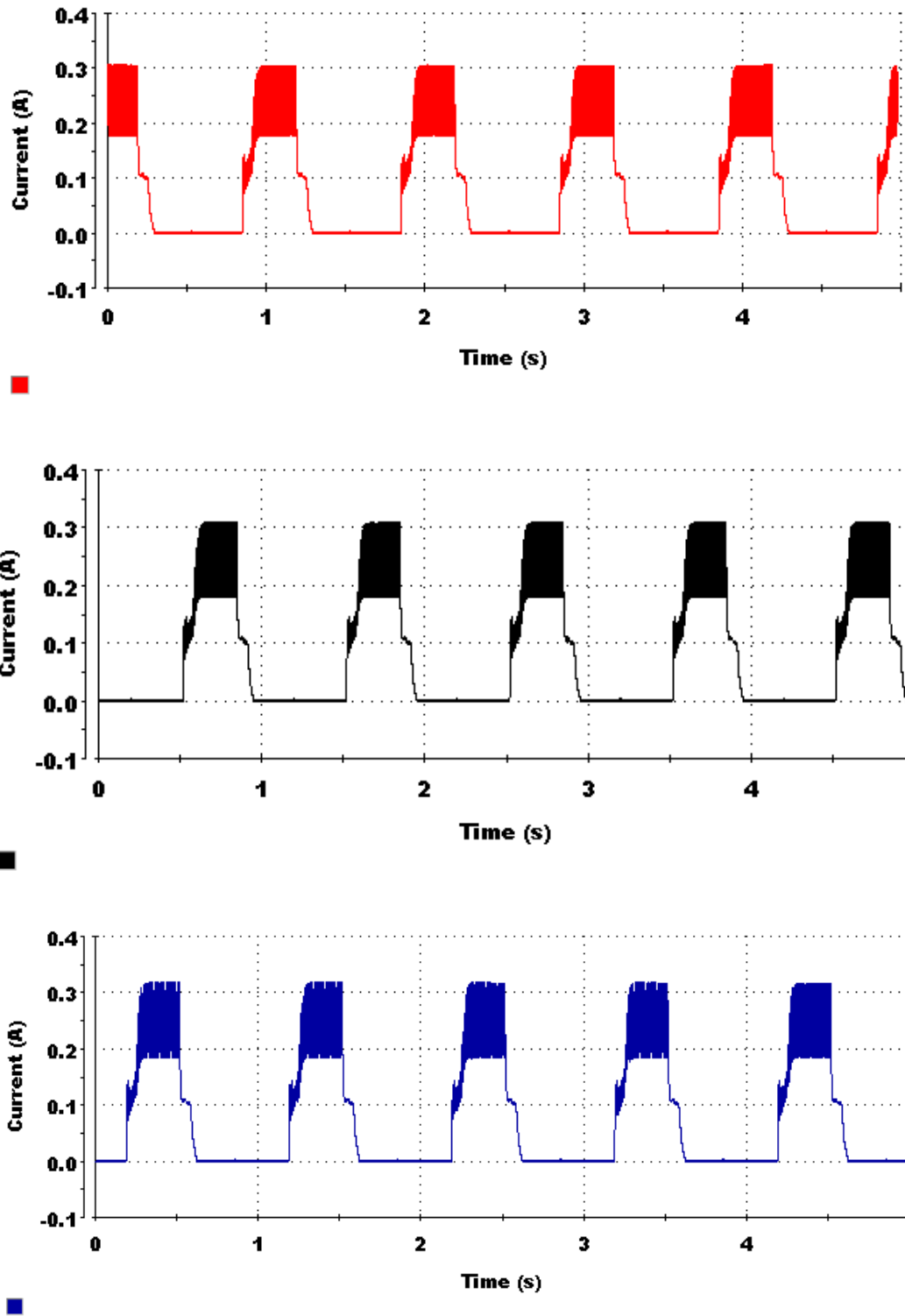


Figure.5.8: Three phase currents A, B, C, open loop performance

Chapter 6

CONCLUSION AND FUTURE WORK

6.1 Conclusions

The outline of this thesis was to build up and to simulate of a practical SRM drive system by using *Matlab / Simulink* and the *dSpace* system. First, a literature study was done about the fundamental operation of *SRM* and then a real *SRM* was disintegrated for estimating its parameters such as aligned and unaligned inductances, number of windings and the other specifications of the machine. After that, these parameters were used in *ANSYS* software to do a simulation performance to compare the practical results of the inductances with the simulated ones.

A linear mathematical model of a 6/4 *SRM* was designed in *Matlab / Simulink* to implement speed controller. In this model a speed controller *PI* with an anti-wind up was used. The values of K_p and K_i were calculated by the crossover frequency f_{cv} and phase margin Ph_m . The dynamic response of the machine was investigated under different working conditions such as no load and loaded operation and results demonstrated that the speed controller could control the actual speed well. Even though a *PI* speed controller has a good speed response and the ability to achieve stability, it was observed they were sensitive to external disturbances. Fig. 4.10 and 4.11 revealed these instabilities.

The core part of this project was to assemble power converter boards. In total three *PCB* were made and assembled. Before the final operation, they were tested to show their functionality properly. Then, switched reluctance motor was operated successfully by these units and controlling command of the *dSPACE* system. Simultaneously, the measurement units such as protection boards, current and voltage transducers were added to protect the drive system during faulty conditions.

6.2 Future work

Analysis of the *SRM* in this thesis was only done for a linear inductance profile, while in practical situations, machine will have a nonlinear behavior due to the effect of magnetic saturation [3]. Therefore, a potential for further research work in this area is vast and a nonlinear mathematical model based on the magnetization characteristics can be developed for further analysis. An open loop control was performed in this research, however a closed loop experiment can be performed later to observe the capability of the speed controller in a real time implementation.

Based on this model, the other controlling methods such as fuzzy logic and neural networks can be developed to make an advanced controlling system.

References

- [1] R.Krishnan,“Switched Reluctance Motor Drives, Modeling, Simulation, Analysis, Design, and Applications”.
- [2] Mohan.Ned, “Electric Drives ,An Integrated Approach” .Minnesota University.
- [3] P.J.Costa Branco, “Dynamic Simulation Models of Switched Reluctance Motor Drivers Based on Matlab/Simulink”.
- [4] Jin-Woo Ahn, “Switched Reluctance Motor Drives” PhD. Thesis Kyungsoong University Korea.
- [5] T. DiRenzo , “Switched Reluctance Motor control” Texas Instruments.
- [6] Michael T. DiRenzo “Speed controlling of Switched Reluctance Motor Drives” Texas Instruments.
- [7] Thomaq KOBLARA “Implementation of Speed Controller for Switched Reluctance Motor Drives” IEEE International conference power electronics and drives.
- [8] T.J.E. Miller “Switched Reluctance Motors and Their Control” Magna Physics Publishing And Clarendon Press, Oxford 1993.
- [9] C. Moron , A. Garcia “Torque cControl of Switched Reluctance Motors” IEEE Transactions on Magnetics, Vol. 48, NO. 4, April 2012.
- [10] Electrical Engineering Laboratories “PID Speed Controller with Anti Wind” Educational materials for motor drives.
- [11] Signals and systems Labarotories “Introduction to Simulink and dSPACE System”
- [12] Nikolay Radimov “Inductance measurements in switched reluctance machines” Department of Electrical and Computer Engineering, Ben-Gurion University of the Negev.
- [13] Huijun Zhou, Wen Din “A Nonlinear Model for the Switched Reluctance Motor” School of Electrical Engineering, Xi'an Jiaotong University, Xi'an 710049, China.
- [14] Gobbi. R Membe “Rising and falling current methods for measurement of flux-linkage characteristics of switched reluctance motors ” First International Power and Energy Coference PECon 2006, November 28-29, 2006, Putrajaya, Malaysia
- [15] Md. Rezaul “Hasan A Comprehensive Model of SRM in MATLAB Environment”International Journal of Engineering & Computer Science IJECS-IJENS Vol:12 No:04
- [16] Paul B. Crilly “A Simulation Model For Four Phase Switched Reluctance Motor”TheUniversity of Tennessee, Knoxville.
- [17] Dr. Ridley “Choosing Crossover Frequency For a Switching Power Supply”, Ridley Engineering.